Journal Pre-proofs

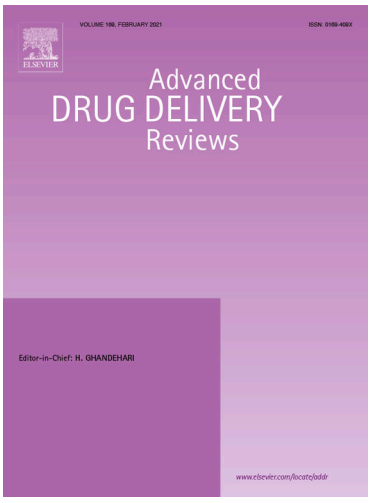

Advances in powder bed fusion 3D printing in drug delivery and healthcare

Atheer Awad, Fabrizio Fina, Alvaro Goyanes, Simon Gaisford, Abdul W. Basit

PII: S0169-409X(21)00153-8
DOI: https://doi.org/10.1016/j.addr.2021.04.025
Reference: ADR 13787

To appear in: *Advanced Drug Delivery Reviews*

Received Date: 28 November 2020
Revised Date: 3 April 2021
Accepted Date: 28 April 2021

Please cite this article as: A. Awad, F. Fina, A. Goyanes, S. Gaisford, A.W. Basit, Advances in powder bed fusion 3D printing in drug delivery and healthcare, *Advanced Drug Delivery Reviews* (2021), doi: https://doi.org/10.1016/j.addr.2021.04.025

Advances in powder bed fusion 3D printing in drug delivery and healthcare

Atheer Awad[1], Fabrizio Fina[1], Alvaro Goyanes[1,2,3*], Simon Gaisford[1,2] and Abdul W. Basit[1,2*]

[1] UCL School of Pharmacy, University College London, 29-39 Brunswick Square, London, WC1N 1AX, UK

[2] FabRx Ltd., Henwood House, Henwood, Ashford, Kent TN24 8DH, UK

[3] Departamento de Farmacología, Farmacia y Tecnología Farmacéutica, I+D Farma (GI-1645), Facultad de Farmacia, and Health Research Institute of Santiago de Compostela (IDIS), Universidade de Santiago de Compostela, 15782 Santiago de Compostela, Spain

*Correspondence: a.basit@ucl.ac.uk (Abdul W. Basit)

a.goyanes@fabrx.co.uk (Alvaro Goyanes)

Abstract

Powder bed fusion (PBF) is a 3D printing method that selectively consolidates powders into 3D objects using a power source. PBF has various derivatives; selective laser sintering/melting, direct metal laser sintering, electron beam melting and multi-jet fusion. These technologies provide a multitude of benefits that make them well suited for the fabrication of bespoke drug-laden formulations, devices and implants. This includes their superior printing resolution and speed, and ability to produce objects without the need for secondary supports, enabling them to precisely create complex products. Herein, this review article outlines the unique applications of PBF 3D printing, including the main principles underpinning its technologies and highlighting their novel pharmaceutical and biomedical applications. The challenges and shortcomings are also considered, emphasising on their effects on the 3D printed products, whilst providing a forward-thinking view.

Keywords:

Additive manufacturing; 3D printed drug products and oral dosage forms; printlets; SLS; SLM; DMLS; EBM; MJF; digital pharmaceutical sciences; personalized pharmaceuticals and medicines; drug delivery systems and prosthetics.

Table of contents

1 Introduction

Three-dimensional (3D) printing is an overarching term that has been used to describe a set of additive manufacturing technologies that build objects from a computer-aided design (CAD) model in a layer-by-layer manner [1-5]. Different types of 3D printing processes have been introduced, with each technology having unique attributes and feedstock materials, making their applications both diverse and distinctive [6-11]. The American Society for Testing and Materials (ASTM) categorises 3D printing processes into seven main groups; vat polymerisation, binder jetting, material jetting, direct energy deposition, sheet lamination, material extrusion and powder bed fusion [12]. Each group is broken down into subsets of multiple printing technologies that typically share the same principles to consolidate feed materials into 3D objects [13-18].

3D printing has recently gained interest in various industries, offering new manufacturing paradigms to production of existing or novel product designs [19-26]. Within the pharmaceutical industry, it is seen as a disruptive technology with the potential to digitalise pharmaceutical production by dispensing individual units of

personalised medications in a flexible manner [27-32], moving treatments away from one-size-fits-all dosing [33-36]. Due to the unique attributes of the 3D printing technologies, such as their additive nature and ability to be combined with 3D imaging, they can be exploited to create 3D objects that are typically challenging to be made using conventional production processes [37-41]. As such, their use for designing and assessing innovative drug-eluting dosage forms is particularly promising for advancing the pharmaceutical sector into digital healthcare [42-45].

Since the approval of the first 3D-printed tablet (Spritam) by the United States Food and Drug Administration (FDA) [46], 3D printing has been evolving rapidly in the pharmaceutical arena, with cutting-edge research demonstrating the unique prospects this technology can offer [47-51]. This has led many researchers to explore and study further 3D printing technologies to evaluate their use within healthcare [52-56]. Powder bed fusion (PBF) is a 3D printing type that uses a focused power source (e.g., laser or electron beam) to selectively consolidate powder particles into solid objects [57, 58]. One key advantage of PBF technologies is their ability to fabricate overhanging geometries without the need for support structures because the loose powder particles inside the printing platform act as a support ensuring the integrity of the printed objects throughout printing. Thus, a variety of complex and highly detailed objects can be produced using PBF and its uses span various industries (e.g., aerospace, automotive, military, medical, dentistry, engineering and electronics) [59-66]. PBF has also been explored for pharmaceutical use, where a feedstock material, constituting a pharmaceutical-grade powder blend of a drug and thermoplastic polymer, has been used. Therefore, in terms of starting materials, PBF is considered to hold the closest resemblance to traditional tabletting processes when compared with other 3D printing

technologies [67]. Moreover, 83% of 3D printed medical devices cleared by the FDA between the years 2010 and 2015 were manufactured using PBF 3D printing, making it more favourable over material extrusion and vat polymerisation 3D printing technologies [68]. Thus, of the different printing technologies, the PBF technologies may be the most suited for use within pharmaceutical research, because they are more feasible to explore and offer a novel and versatile approach for the rapid tailoring of devices and medications.

This review article outlines the main principles underpinning PBF 3D printing technologies, highlighting their unique inherent properties and discussing the differences between them. The recent applications and advantages of PBF within healthcare are also provided. And finally, an insight into the technical challenges and in-process conditions affecting the final 3D object are discussed.

2 The technologies

Currently, PBF is classified into four subset technologies; selective laser sintering (SLS), selective laser melting (SLM) / direct metal laser sintering (DMLS), electron beam melting (EBM) and multi-jet fusion (MJF) (Figure 1) [69]. A summary of the different PBF technologies is shown in **Table 1**. Generally, all the PBF technologies share the same underpinning principles that include building objects in a layer-by-layer fashion using thermal energy resulting from the combination of increased temperature and the use of an energy source [70]. Moreover, all the PBF technologies use powdered feedstock materials, where the main differences between them lie in the type and amount of energy transmitted to the powder bed for consolidation and in the type of powdered materials they employ. For instance, whilst SLS, SLM and DMLS

employ a laser beam and EBM uses an electron beam, MJF functions using an infrared lamp. In the same vein, the feed materials in SLM and DMLS include metals or alloyed powders [71], whereas thermoplastic polymers are used in the case of SLS and MJF.

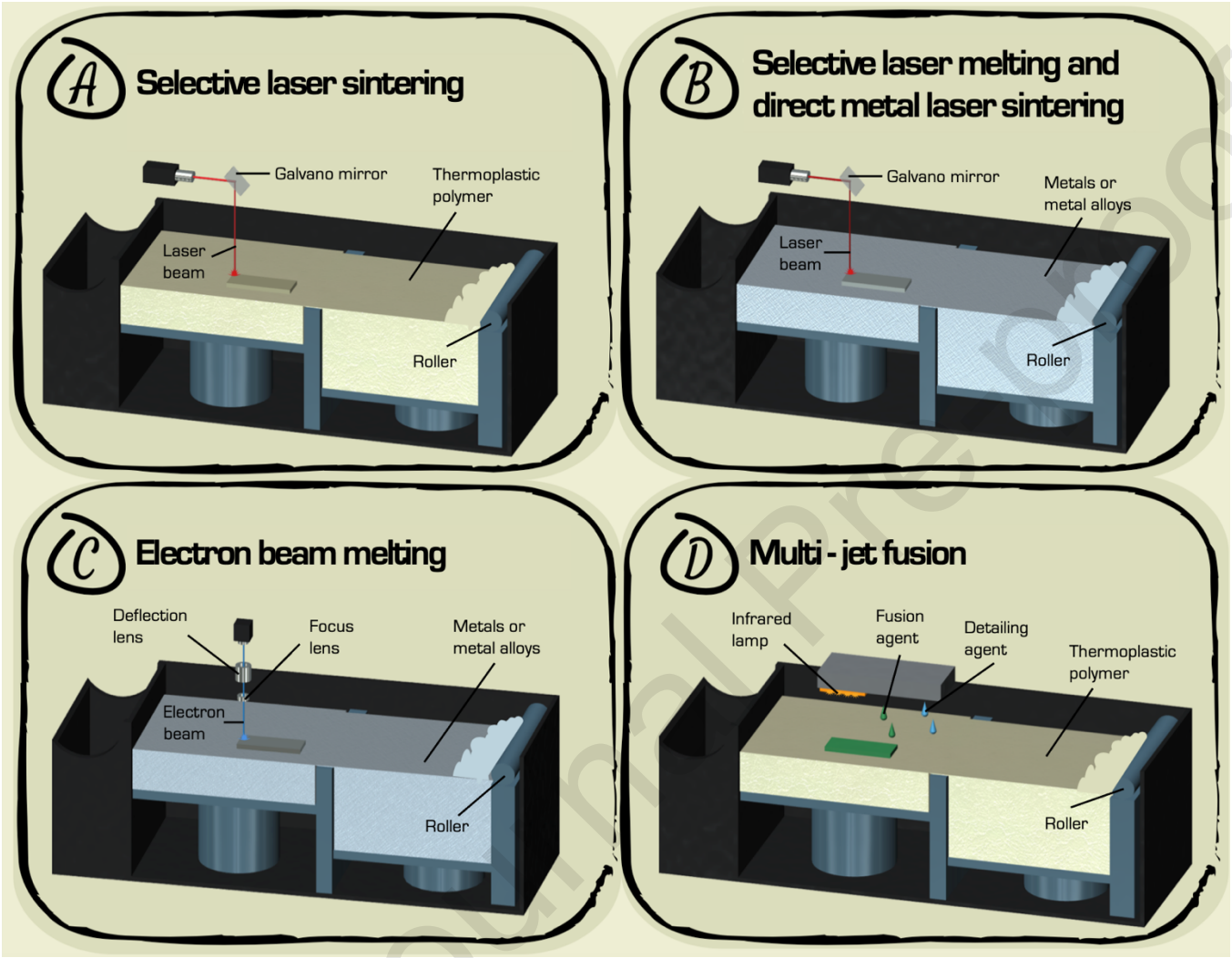

Figure 1. Graphical illustration of (A) selective laser sintering, (B) selective laser melting and direct metal laser sintering, (C) electron beam melting and (D) multi-jet fusion 3D printing technologies.

Table 1. A summary of the different powder bed fusion (PBF) technologies, highlighting the similarities and differences between them; *SLS, selective laser sintering; SLM, selective laser melting; DMLS, direct metal laser sintering; EBM, electron beam melting; MJF, multi-jet fusion*.

Technology	**Energy source**	**Power (kW)**	**Feedstock material**	**Powder particle size (μm)**	**Layer thickness (μm)**	**Build speed (mm/h)**	**Reference(s)**
SLS	Laser beam	Up to 0.04	Thermoplastic polymers	58-180	100-120	4.2 - 20	[67, 72-74]
SLM/DMLS	Laser beam	Up to 1	Metals / alloyed powders	20-63	20-100	7 - 8	[75]
EBM	Electron beam	Up to 60	Metals / alloyed powders	45-150	50-200	6 - 7	[75]
MJF	Infrared lamp	-	Thermoplastic polymers	35-120	70-100	1.8 - 4	[72, 76-78]

As shown in **Figure 1**, the PBF systems are typically comprised of five main parts; (i) a build platform/tank, where objects are printed; (ii) an energy source, which is responsible for the consolidation process; (iii) a powder reservoir platform/tank or hopper, where fresh powder is held before being dispensed onto the building platform; (iv) a mechanical roller, that spreads the fresh powder onto the building platform and flattens it; and (v) a material container, which is responsible for recovering and recycling loose powder material. The PBF printing process involves raising the build platform to its highest level. Then, a fresh layer of powder is dispensed and flattened by the roller [79]. The energy source is then activated, which selectively scans across the powder in the build platform, consolidating the powder particles based upon the pattern from the 3D file. Thereafter, the build platform moves down to create sufficient space for a new powder layer. This is followed by the rising of the reservoir platform and the spreading of a new layer of powder by the roller. This process is then repeated until the printing job has been completed [80]. At the end of the process, the 3D printer is left to cool down, after which the loose powder particles are brushed off or removed with compressed air to recover the printed 3D object. In some cases, the printed object may need to be coated, polished or undergo surface finishing to enhance its mechanical properties or improve its appearance.

Due to its ability to employ different types of materials and 3D designs, PBF 3D printing can be exploited in a wide array of industries, with its applications extending to electronics (Figure 2A), automotive and aviation industries (Figure 2B), explosives, medical implants (Figure 2C), surgical tooling, tissue engineering and dental prosthetics and appliances (Figure 2D) [81].

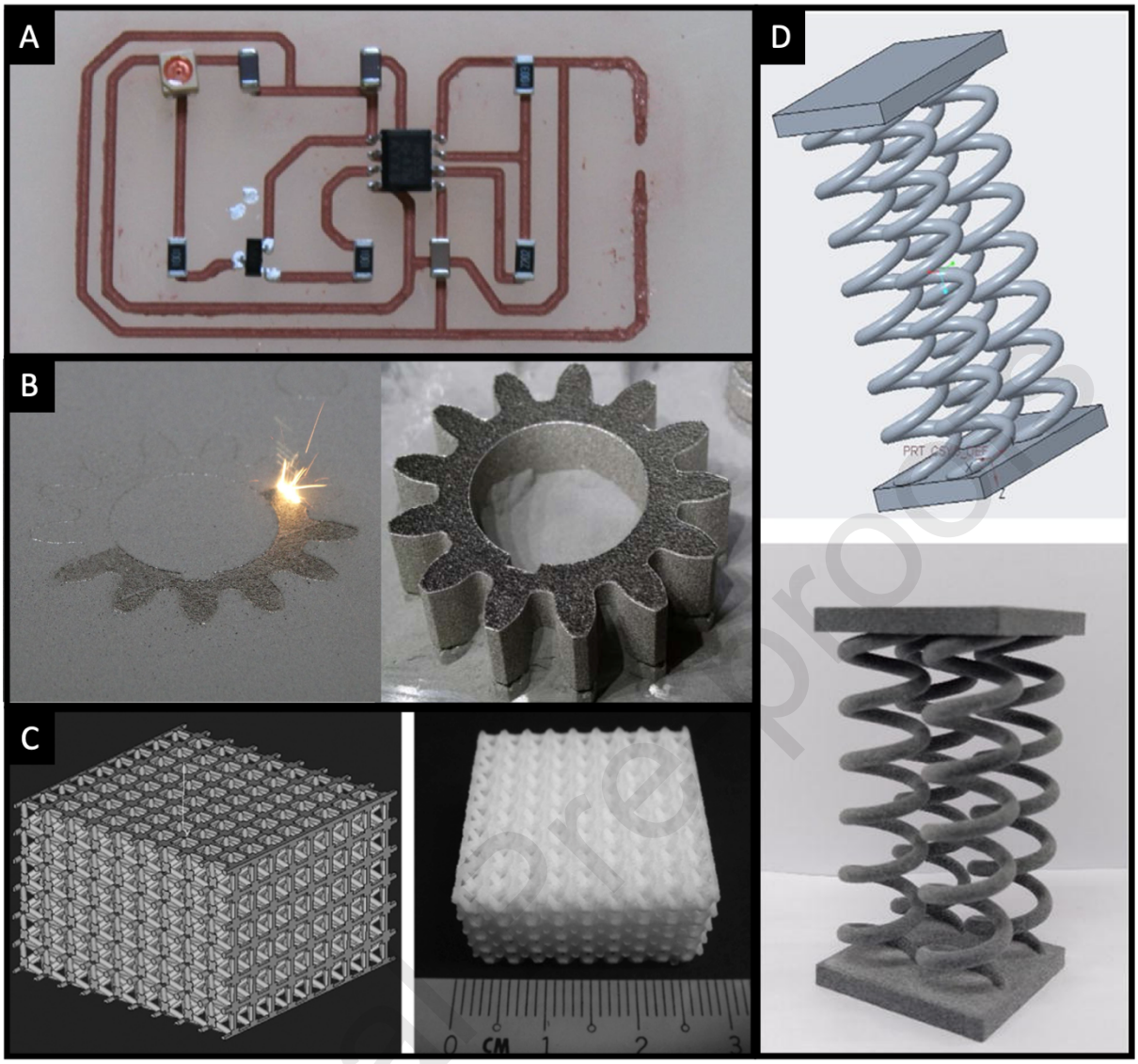

Figure 2. (A) Image of SLM printed circuit. Reprinted with permission from [82]. (B) Image of a DMLS 3D printed aircraft engine transmission gear (left) during printing and (right) following post-processing. Reprinted with permission from [83]. (C) (left) 3D design and (right) image of an SLS 3D printed scaffold with a polyhedral structure for bone regeneration. Scale shown in cm. Reprinted with permission from [84]. (D) (top) 3D model and (bottom) image of a helical spring–based lattice structure fabricated using MJF. Reprinted with permission from [85].

3 Healthcare applications of PBF

To understand the main differences between the different PBF technologies and their unique applications within healthcare, each technology will be discussed in more detail.

3.1 Selective laser sintering (SLS)

SLS 3D printing utilises a laser beam to fuse powder particles together at their surfaces, a process termed 'sintering' (Figure 1A) [86, 87]. This technology was developed by Carl Deckard in 1984, with the first model employing a neodymium-doped yttrium aluminium garnet (Nd:YAG) laser [88]. Nowadays, SLS 3D printers employ a variety of laser types, including diode, fibre and carbon dioxide (CO_2) lasers, with the latter being the most common type.

Owing to initial suspicions of drug and/or excipient degradation being caused by the laser [89], early uses of SLS in pharmaceutical research did not include any drug substance but instead, a methylene blue dye was used [90]. Porous nylon cubes (8 x 8 x 8 mm) were fabricated by adjusting the laser power and scanning speed of a CO_2 laser. It was demonstrated that as the laser scanning speed increased, the porosity of the printed objects increased. In the case of laser power, as it increased the porosity of the object decreased. A following study showed that both porosity and drug release could be controlled by repositioning dense walls in the 3D printed drug delivery devices [91]. This was achieved by re-orienting the 3D designs of the devices, thus changing their 3D printing pattern. Subsequently, the first attempt to employ biodegradable polymers for SLS use involved the use of polycaprolactone (PCL) and poly-L-lactide (PLLA) [73]. The printing conditions were optimised to create porous drug delivery devices with strong mechanical characteristics. In particular, two printing parameters,

the laser scanning speed and laser power, were used to control properties of the devices. In another approach, the exterior structure of the devices was used to control the drug release [92]. To reduce the burst release, the dwell of the laser was used to include additional barrier rings on the exterior of the devices; the addition of more barriers resulted in a more significant reduction in the burst release.

Despite the promising results, the early studies did not evaluate the effect of the laser energy on the drug stability. Thus, doubts relating to the suitability of SLS 3D printing for pharmaceutical use persisted. This was the case until 2017, when the first SLS Printlets™ (3D printed tablets) were fabricated [93]. Herein, a diode laser was investigated for pharmaceutical SLS printing for the first time. The Printlets incorporated paracetamol as a model drug and were fabricated using two commercial pharmaceutical grade polymers; Eudragit L100-55 and Kollicoat IR. Due to the intrinsic properties of the polymers, the Eudragit L100-55 Printlets displayed prolonged release characteristics, whilst those incorporating Kollicoat IR had immediate release characteristics. To eliminate any concerns relating to drug degradation resulting from the diode laser, degradation studies were performed and confirmed that no drug degradation has occurred. Another important finding of this study was that sintering could not occur when using a feedstock consisting of the polymer and drug mixture solely, as the use diode laser emitted its energy in the visible light region. Since most pharmaceutical powders are white in colour, no energy absorption from the laser occurred. As such, a suitable solution to this problem involved the incorporation of a pharmaceutical grade colourant into the feedstock powder mixture, facilitating absorptance of the energy emitted from the diode laser.

With its unique features, SLS 3D printing offers a wide range of novel pharmaceutical applications. For instance, (i) SLS has the ability to create free-form 3D objects without the need for additional support materials; (ii) the capacity of the SLS build platform can be increased and its productivity enhanced by stacking printed objects on top of one another, making it more amenable for scale up and mass production compared with other 3D printing technologies; (iii) SLS can create objects with high degrees of porosity and pore connectivity [94]; (iv) there is no need for pre-processing SLS feedstock materials, which is a necessity in the case of other 3D printing technologies (e.g., fused deposition modelling (FDM) requires the creation of filaments); (v) the process does not involve the use of solvents, and thus is considered safe for use with drugs that are prone to hydrolysis; (vi) SLS enables the recycling and reprocessing of feedstock materials, which reduces production waste and supports green pharmaceuticals; (vii) it does not require additional excipients that could lead potential toxicities; and (viii) SLS has shown to be more cost effective for the production of personalised parts compared to other 3D printing technologies (e.g., fused deposition modelling (FDM) and stereolithography (SLA)) and conventional pharmaceutical production processes (e.g., injection moulding) [95, 96]. Collectively, these properties make SLS 3D printing a highly flexible technology that is suited for the preparation of a variety of pharmaceutical dosage forms and medical devices.

Because SLS permits the use of feed materials with distinctive intrinsic characteristics, an array of drug release modes can be attained. This can be achieved by modulating the printing parameters and carefully choosing a suitable polymer matrix. As an example, selecting an immediate-release polymer matrix (e.g., Kollicoat IR (Figure 3A) [93] or hydroxypropyl methylcellulose (HPMC) (Figure 3B) [97]) allows the production

of Printlets with instant release patterns. On the other hand, selecting a polymer with pH-dependent properties (e.g., Eudragit L100-55 (Figure 3A) [93]) or sustained release properties (e.g., PCL and PLLA (Figure 3C) [73]) yields Printlets with controlled release properties. The Printlets can be loaded with various drug percentages, wherein a different drug content will change the energy absorption of the feed powder and the mechanical properties, and thus will result in Printlets with different drug release characteristics. As an example, in one study, increasing the paracetamol content in the Printlets (e.g., 5% to 35%) resulted in a higher degree of consolidation and stronger interparticle connections. This in turn slowed down the rate at which the dissolution medium penetrated into the Printlets and decelerated the drug release (Figure 3A) [93]. However, this observation was specific to paracetamol and other drug substances and powder mixtures may display different effects. Laser absorption can also be controlled by changing the laser scanning speeds, which can also be used to modulate the drug release properties [97]. As an example, at laser scanning speeds of 100, 200 and 300 mm/s, paracetamol Printlets with a HPMC matrix have shown to achieve a complete drug release within 4 h, 3 h and 2 h, respectively (Figure 3B). This is because as the laser scanning speed decreases, the contact time between the laser beam and the powder bed increases, resulting in a higher degree of consolidation and hence, a slower drug release. The use of SLS has also shown to give amorphous solid dispersions, without the need for further post-processing [98]. This in turn improves the solubility of poorly soluble drug agents and enhances their bioavailability.

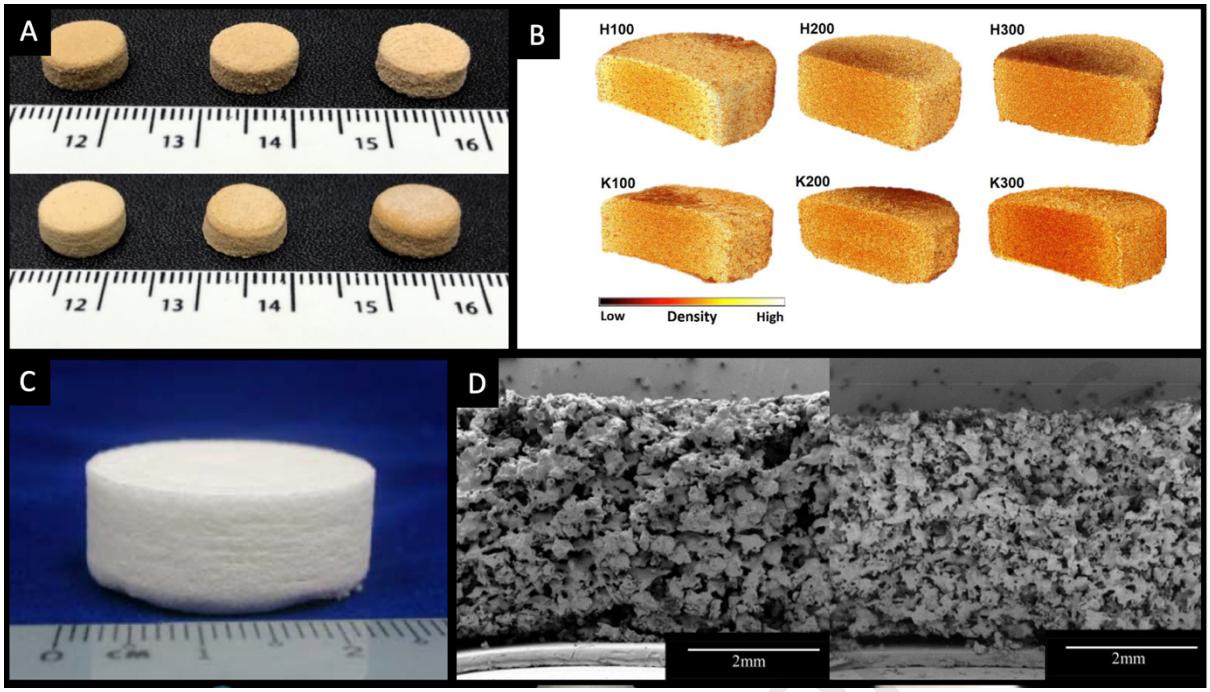

Figure 3. (A) Image of the (top) Kollicoat IR and (bottom) Eudragit L100-55 Printlets, incorporating (from right to left) 5, 20 and 35% paracetamol, respectively. Scale shown in cm. Reprinted with permission from [93]. (B) X-ray micro-CT images on cross sections of the (top) HPMC and (bottom) Kollidon VA64 Printlets fabricated at a laser scanning speed of (from left to right) 100, 200 and 300 mm/s, respectively. The coloured scale bar represents density. Reprinted with permission from [97]. (C) Image of a PCL-based SLS 3D printed tablet. Scale shown in cm. Reprinted with permission from [73]. (D) Surface electron microscopy (SEM) cross-sectional images of the orally disintegrating ondansetron Printlets, containing (from left to right) 50 and 60% mannitol, respectively. Reprinted with permission from [99].

Orally disintegrating and fast-dissolving Printlets can also be created using SLS 3D printing. This can be achieved by exploiting the technology's ability loosely to bind powder particles on the surface. As the process does not involve the use of compression forces, the resulting Printlets are highly porous. In the presence of even small volumes, the liquid can rapidly penetrate into the Printlets, breaking them into

small fragments. This outcome can be modulated by controlling the laser scanning speed, wherein the disintegration speed can be further increased by utilising a higher laser scanning speed [97]. This is because as the laser scanning speed increases, the contact time between the laser beam and powder bed surface decreases. As a result, Printlets with rapid disintegration properties are created whilst maintaining acceptable mechanical characteristics. However, this requires the use of a polymer matrix with rapid disintegration properties. As an example, paracetamol and ondansetron Printlets based on a Kollidon VA64 matrix have shown to have disintegration times varying at >600, 15 and 4 s, when printed at laser scanning speeds of 100, 200 and 300 mm/s, respectively (Figure 3B and 3D) [97, 99]. Because of that, Printlets fabricated at a speed of 100 mm/s achieved complete drug dissolution within 1 h, whilst those printed at speeds of 200 and 300 mm/s required only 5 min for the complete dissolution. In a succeeding study, it was shown that the incorporating 30% diclofenac sodium as the drug substance resulted in a slow disintegration rate and altered the mechanical properties of the Printlets when compared with those incorporating paracetamol [100]. Thus, to improve the mechanical characteristics and speed up the disintegration time of the Printlets, lactose monohydrate was incorporated into the formulation. A similar approach was used in a following study, wherein a mixture of lactose monohydrate and microcrystalline cellulose was used [101], with clindamycin palmitate HCl used as the drug agent.

SLS orally disintegrating Printlets have shown to offer an innovative and practical way to deliver medications suited for patients with visual impairment [102]. This is because the Printlets disintegrate within ~5 s, avoiding the need for being taken with water and thus facilitating self-administration of medications. To suit the needs of this patient

group, the 3D design of the Printlets can be modified to include Braille and Moon patterns on their surfaces, permitting patients to identify medicines using tactile perception (Figure 4A). This is particularly useful when medications are taken out of their original packaging. Moreover, Printlets with innovative shapes (e.g., sun, moon, heart, caplet shape, pentagon and square) can be fabricated to enable the inclusion of additional medication information (e.g., medication indication and/or dosing regimen). For example, a heart shape can be used to refer to medications used to treat cardiovascular conditions. In the same vein, the sun and moon shapes can be used as a reference to morning and evening dosing regimens, respectively. The number of flat sides in a pentagon and a square can be used to correspond to the medication dosing time. The study has shown that up to three Braille letters can be printed onto bigger sized formulations (e.g., a caplet shape), which can be used for three-letter abbreviations. For instance, PAR can be used as an abbreviation for paracetamol (Figure 4A). The use of these Printlets in patients with visual impairment may aid in reducing medication errors and improving adherence to treatments.

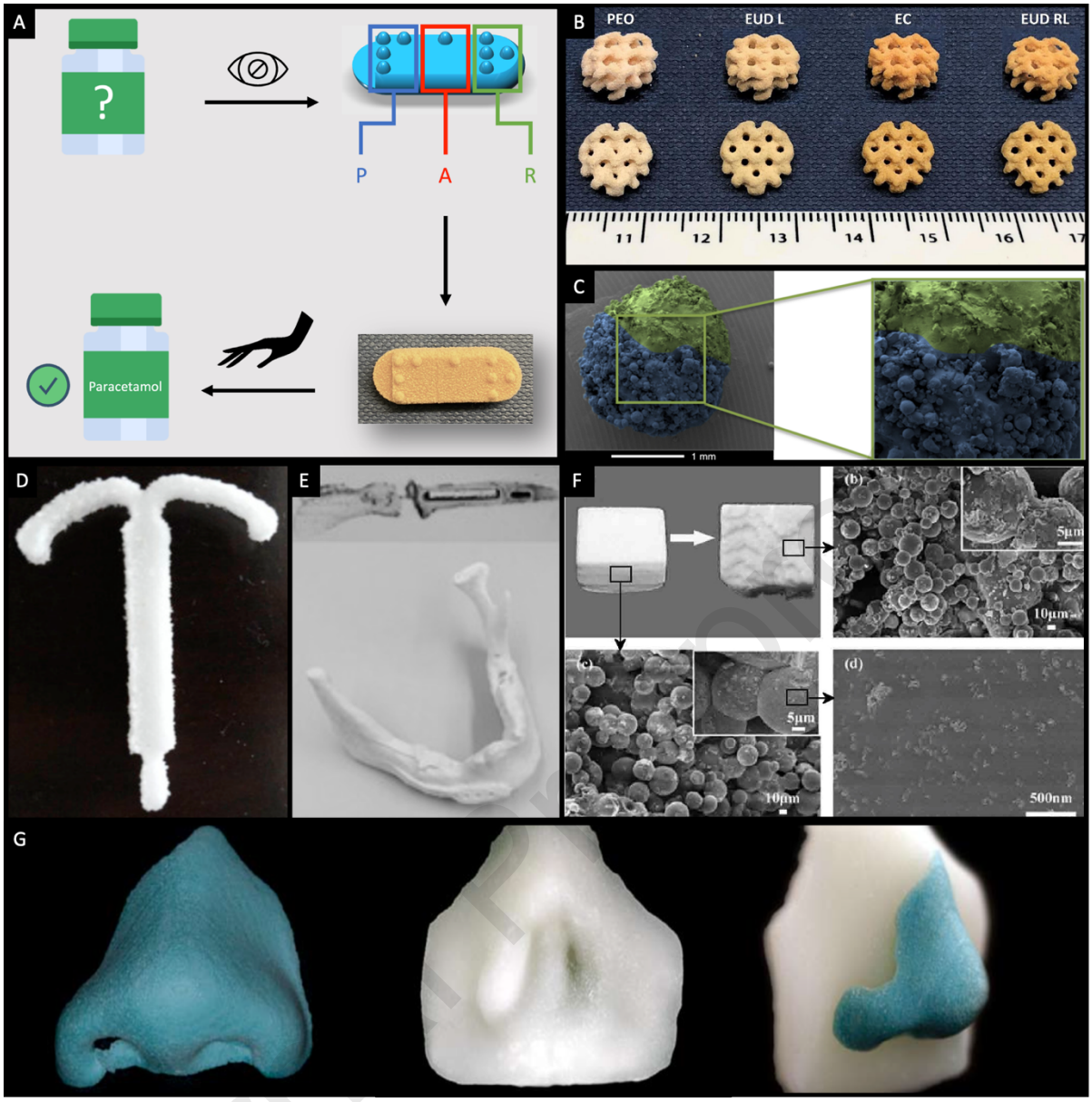

Figure 4. (A) Graphical illustration showing how SLS Printlets incorporating three Braille letter abbreviations can be used by visually impaired patients to identify medications. Reprinted with permission from [102]. (B) Images of SLS gyroid lattice Printlets fabricated using (from left to right) polyethylene oxide, Eudragit L100-55, ethyl cellulose and Eudragit RL. Scale shown in cm. Reprinted with permission from [103]. (C) SEM image of a dual SLS mini-Printlet, where the blue colour represents the Kollicoat IR matrix and the green colour represents the ethyl cellulose matrix. Reprinted with permission from [104]. (D) Image of an SLS 3D printed intrauterine

device. Reprinted with permission from [105]. (E) Image of a smart mandible implant with an embedded drug delivery system. Reprinted with permission from [106]. (F) Image and SEM micrographs of an SLS 3D printed cube. Reprinted with permission from [107]. (G) Image of (from left to right) wax model of nasal prosthesis, resin model of nasal defect and wax nasal pattern with resin model, all fabricated using SLS 3D printing. Reprinted with permission from [108].

The high resolution of its laser beam allows SLS 3D printing to be used for creating complex structures (e.g., multi-reservoir systems [109]), enabling controlled delivery of drugs. The release of progesterone from these systems can extend over a period of 290 days depending on their content [110]. The loose powder particles inside the SLS printing platform can be used as rafts to support objects during the printing process and maintain their integrity. This, along with the high-resolution laser, allows the fabrication of intricate Printlets (e.g., gyroid lattices (Figure 4B) [103]), enabling the fine-tuning of the drug release pattern. Compared with cylindrical Printlets, the gyroid lattices exhibit a more rapid drug release behaviour. As the 3D printing processes occur in a layer-by-layer fashion, it is possible to create bi-layer Printlets that combine gyroid lattice and cylindrical structures, enabling higher control over the drug release pattern. Similarly, 3D printed pellets, termed mini-Printlets, can be prepared using SLS 3D printing [104]. These mini-Printlets offer a universal platform for delivering personalised medication doses. Herein, SLS 3D printing offers a single step method to create controlled-release multiparticulate systems, which normally are laborious and expensive to produce, requiring multi-step processes that involve the use of dedicated equipment [111]. In addition, the use of SLS aids in regulating the initial drug release. This is due to the strong coherence between the drug and polymer

particles that results from the sintering process, which in turn induces a sustained effect. Dual mini-Printlets that combine two spatially separated drug agents (e.g., paracetamol and ibuprofen) with individualised release characteristics can also be fabricated by modulating the composition of the polymer matrices (Figure 4C). This provides an innovative and flexible platform that can be used for multi-drug therapy in different patient groups, which can be dosed conveniently and provide long-term therapeutic effects. In this novel drug delivery system, each mini-Printlet functions as a separate drug system. Thus, the risks of dose-dumping and peak plasma fluctuations are lower compared to monolithic pharmaceutical dosage forms.

Another example that demonstrates SLS's unique ability to overcome geometry limitations imposed by traditional production processes is its use for creating intrauterine devices containing two drug substances (e.g., progesterone and 5-fluorouracil) (Figure 4D) [105]. The two drugs have shown synergism when used to treat endometrial and ovarian cancers. Progesterone exhibited zero-order kinetics, whereas 5-fluorouracil displayed an initial burst release after 1 h, followed by a sustained release extending up to 35 days. The devices were fabricated using two different laser powers, 3 W and 5 W, wherein a high drug release rate was observed with the devices fabricated using 3 W. This was attributed to the higher porosity resulting at 3 W, which accelerates the drug diffusion. SLS 3D printing was also explored for tissue and bone regeneration, wherein PCL implants incorporating ibuprofen were investigated [112]. The implants containing ibuprofen have been shown to undergo a higher degree of sintering intensity compared with those fabricated using PCL alone. Similarly, 5-fluorouracil implants based on polyethylene (PE) [113] or PCL [114] matrices were studied as a type of cancer treatment. Both

types of implants presented an initial drug release burst followed by a sustained release, with the PE implants having more prolonged effect. Smart mandible implants with embedded drug delivery systems were also be fabricated using SLS 3D printing (Figure 4E) [106]. More recently, cubic-shaped poly(lactic acid) (PLA) and hydroxyapatite (HAP) implants were fabricated for bone repair (Figure 4F) [107]. The implants were biocompatible and displayed favourable osteogenic effect in rats. Nasal prosthesis presents another application for SLS (Figure 4G) [108]. Whilst these prosthesis did not contain any drug agents, similar ones fabricated using FDM and SLA have been suggested for the treatment of acne [115] and as nasal wound dressings [116].

3.2 Selective laser melting (SLM) and direct metal laser sintering (DMLS)

Like SLS, the SLM and DMLS processes utilise a system composed of lenses and Galvano-mirrors to direct the laser beam to a specific position (Figure 1B). Once directed onto the powder bed, the laser beam heats the powder bed and photons are absorbed by the particles, causing them to melt or fuse [117]. Different types of metal granules can be used, including stainless steel, cobalt chrome, aluminium, titanium and tool steel. The main difference between SLM and DMLS technologies is that SLM uses a single component metal (e.g., pure aluminium) and completely melts it at a single melting temperature [118]. In the case of DMLS, the feed powder is generally composed of metal alloys (e.g., titanium alloy) with different melting temperatures. Thus, the process involves the use of high temperature to fuse the powder molecules together.

SLM has been used to fabricate metallic femoral stems for total hip replacement [119]. In terms of drug delivery, due to the high-energy laser beam and elevated temperatures associated with SLM, the process does not allow the direct printing with drugs incorporated in the feed powder. Instead, the drug substance is incorporated following the printing process or is printed using a complementary 3D printing technology. As an example, SLM can be used to print with metals (e.g., cobalt–chromium–molybdenum alloy and titanium alloy) and combined with FDM to print using biodegradable polymers (e.g., polylactic acid) to create implants incorporating both materials (Figure 5A) [120]. The polymer can be loaded with antibiotics (e.g., gentamicin [121]) and embedded within the metallic parts of the implant. As the polymer degrades, the antibiotic is released in a controllable manner during the regeneration of bone cells.

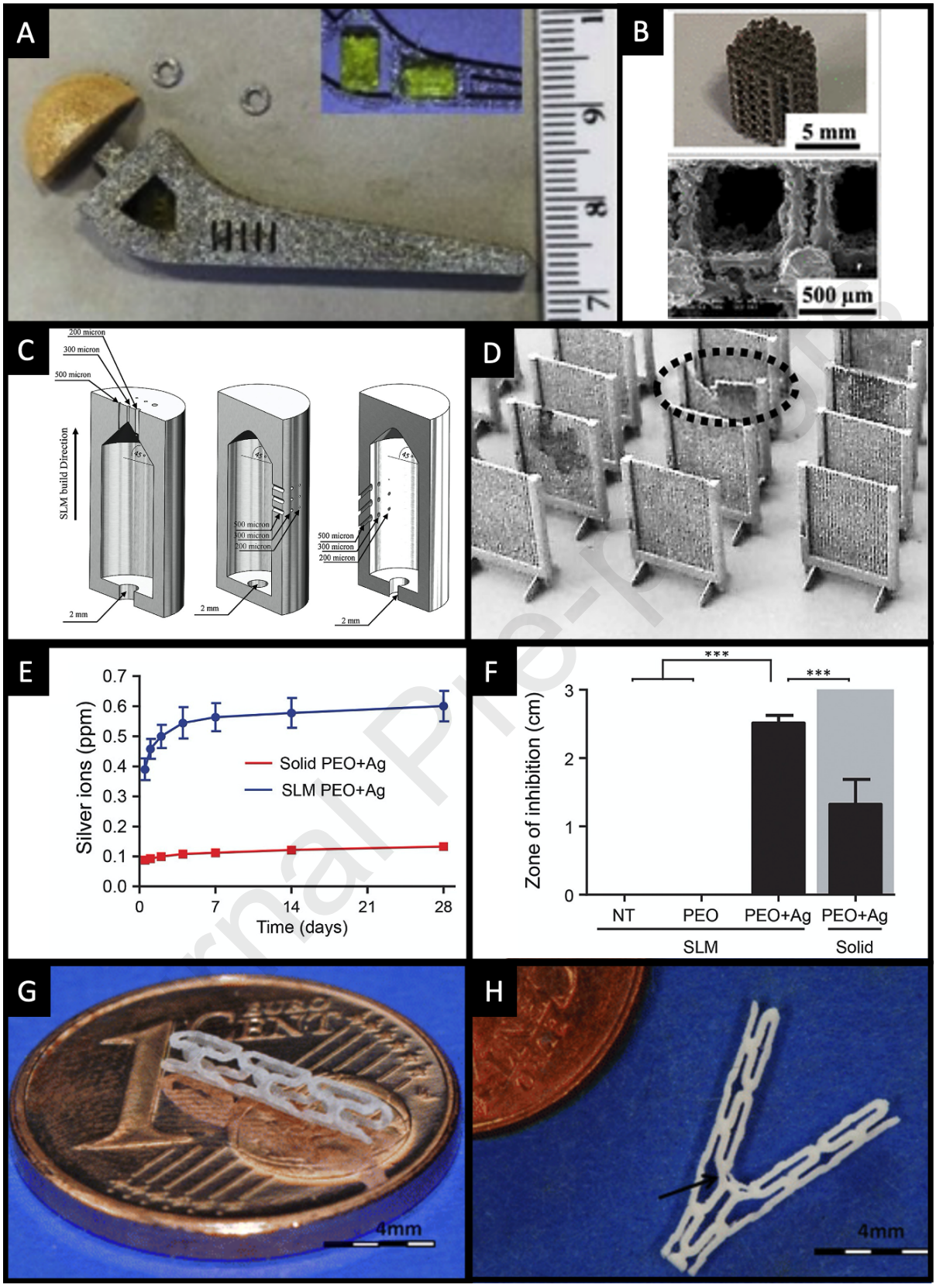

Figure 5. (A) Image of a 3D printed hip implant made using a combination of SLM and FDM 3D printing. The image on the top right corner is a cross-section that shows the

biodegradable polymer embedded within the metallic part. Reprinted with permission from [120]. (B) (top) Image and (bottom) SEM image of porous scaffold for bone regeneration with a 640 μm pore size. Reprinted with permission from [122]. (C) Cross-sectional view of the 3D design of SLM printed titanium implants with (from left to right) vertical channels, horizontal channels and inclined channels. Reprinted with permission from [123]. (D) Images of the orthopaedic SLM 3D printed implants having 400 μm permeable thin walls. Reprinted with permission from [124]. (E) Cumulative silver ion release profiles (n = 3) from the SLM printed and solid implants, measured using ICP-OES. (F) Diameters of the inhibition zones (n = 3) surrounding implants against methicillin-resistant *Staphylococcus aureus* (MRSA) AMC201, measured using a Petrifilm assay; Ag, silver ions; PEO, plasma electrolytic oxidation; ICP-OES, inductively coupled plasma optical emission spectrometry; NT, non-treated. Reprinted with permission from [125]. Image of an SLM 3D printed (G) expandable stent and (H) Y-shaped stent, both fabricated using poly-L-lactic acid (PLLA). Reprinted with permission from [126].

Highly porous titanium alloy scaffolds for bone regeneration were fabricated using SLM 3D printing (Figure 5B) [122]. The scaffolds have shown an interconnected porosity more than 70%, and the pore sizes of the scaffolds altered their osseointegration ability. While in this example no drug was incorporated into the scaffolds, the intrinsic antibacterial activity of titanium alloys could be exploited to prevent infections from occurring during bone regrowth [127, 128]. SLM 3D printing has also been used to fabricate titanium implants with controllable drug release kinetics (Figure 5C) [123]. The drug was added to the implants following the printing process to avoid any degradation. By changing the processing parameters (e.g., laser

power, scanning speed and hatch spacing) and the diameter and position of the microchannels inside the implants, the drug release pattern can be fine-tuned to achieve the desired kinetics. Orthopaedic titanium implants incorporating vancomycin were also fabricated to prevent postoperative periprosthetic joint infections (Figure 5D) [124]. The drug solution was directly injected into the hollow reservoirs following the printing process. Herein, the porosity of the implants was used to regulate the drug release pattern. The implants showed strong antimicrobial activity against *Staphylococcus aureus* with the effective concentrations observed within 5 h and extending for up to 18 h. Likewise, paracetamol- and ciprofloxacin-functionalised titanium implants were also produced using SLM 3D printing [129, 130]. Following the printing process, the drug attachment was achieved using phosphonic acid based self-assembled monolayers. Paracetamol has been shown to adhere to the surface of the implants for up to 4 weeks, after which it was gradually released. In the case of ciprofloxacin, 40% of the drug content still adhered to the implants after 6 weeks.

In another study, SLM titanium implants for bone regeneration were fabricated incorporating silver nanoparticles [125]. The nanoparticles were embedded within an oxide layer that was created using plasma electrolytic oxidation. The implants displayed strong antimicrobial activity, with silver ions exhibiting a constant release over a period of 28 days (Figure 5E). Due to their high porosity, the number of silver ions released from the SLM implants was four times that typically released from analogous solid metallic implants. Similarly, the antimicrobial inhibition zone resulting from the porous implants was double the size of the inhibition zone of the corresponding solid implants (Figure 5F), indicating the SLM implants had a stronger antimicrobial activity. SLM has also been proposed as a viable method for the

fabrication of biodegradable coronary stents (Figures 5G and 5H) [126]. Although the stents did not contain any drug agent, it was suggested in the study that a drug can be incorporated by means of dipping or coating. In particular, drugs such as antiproliferative agents (e.g., Sirolimus) can be used in early stages of stent placements, whilst proendothelial mediators can be used in the advanced stages.

DMLS has been used to create titanium scaffolds for bone regeneration. Here, the scaffolds were used to inhibit bacterial growth without the addition of a drug substance [131]. In another study, a DMLS customised mesh composed of titanium was designed for bone augmentation (Figure 6A) [132]. The meshes were designed based on data collected from computed tomography (CT) imaging. This approach has been shown to be efficient at reducing the time needed to perform surgery, minimise the augmentation volume, reduce risks of errors and improve the quality of treatment. Similarly, a DMLS implant has been used for craniofacial reconstructive surgery [133]. The titanium implants were highly dense with mechanical testing showing they outperformed implants made using annealing. Compared with implants fabricated using conventional production methods, those made with DMLS were able to restore anatomical structure more accurately, even in the case of complex geometries, achieving improved aesthetic appearances [134]. To permit the loading of antibiotics onto DMLS implants, a multi-layer coating approach was used (Figure 6B) [135]. In particular, hyaluronic acid chitosan films incorporating minocycline were self-assembled onto titanium implants following printing using phase-transited lysozyme. The implants promoted bone regeneration whilst preventing bacterial colonisation.

The use of DMLS is not only limited to manufacturing drug delivery systems but can also extend to include creating equipment for drug synthesis. As an example, DMLS was used to create a baffle disc embedded inside a flow distributor for a microreactor assembly (Figure 6C) [136]. The newly proposed microreactor was successful at scaling up the production of an expensive drug, rufinamide, in a single step. This system has shown to be highly productive and cost-effective, making a feasible approach to produce drug substances on-demand.

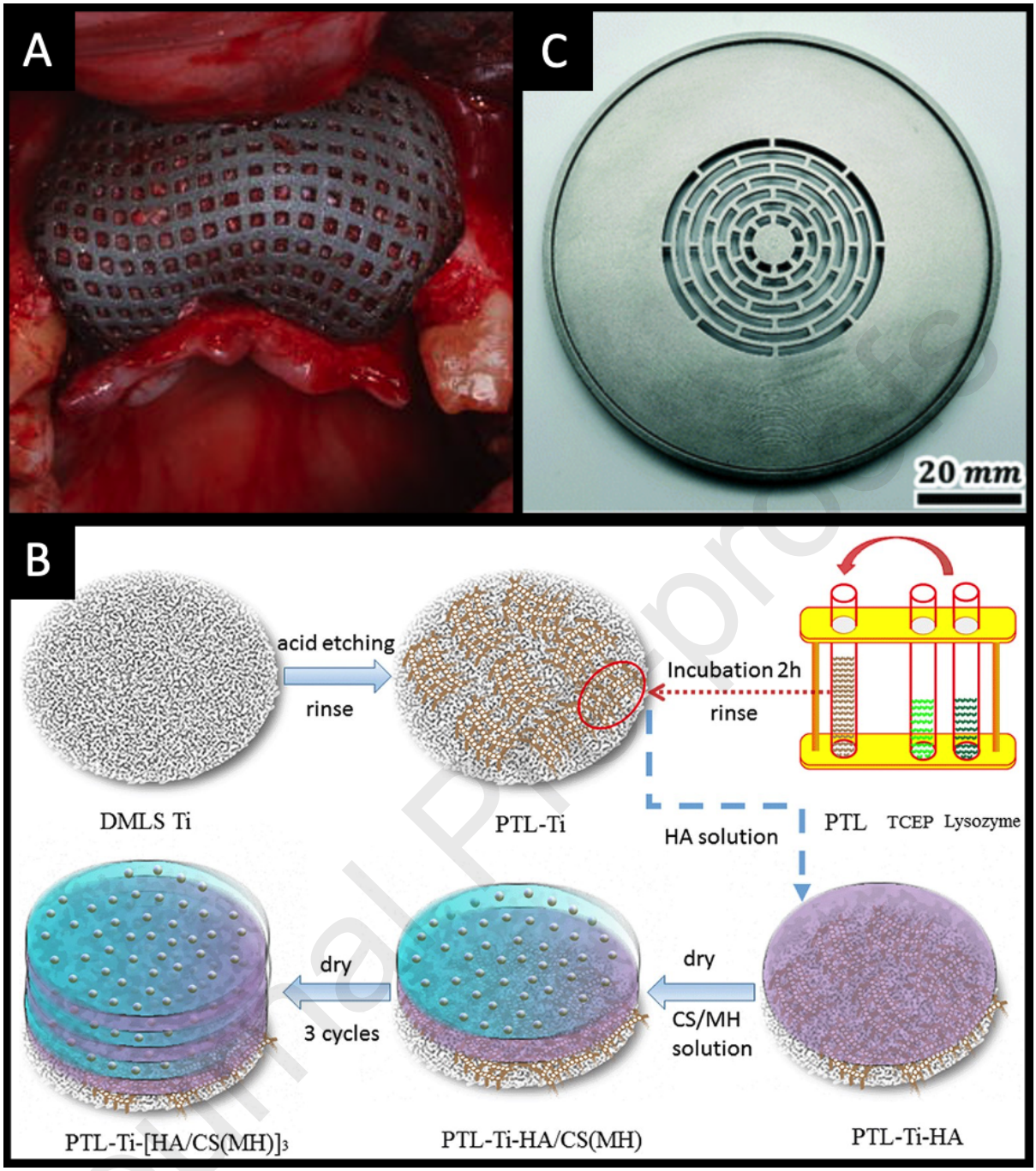

Figure 6. (A) Image of DLMS titanium mesh for bone augmentation. Reprinted with permission from [132]. (B) Schematic diagram showing the process of fabricating minocycline-loaded HA/CS multilayers coating and their assembly onto the surface of DMLS implants. Reprinted with permission from [135]. (C) Image of a DMLS 3D printed baffle disk made out of titanium. Reprinted with permission from [136].

3.3 Electron beam melting (EBM)

In EBM, the energy needed for printing is supplied from an electron beam rather than a laser beam (Figure 1C) [137]. The high intensity of the electron beam renders powdered materials completely molten during the printing process, with temperatures reaching up to 1000 °C [138]. The EBM process entails using a filament, typically made of tungsten, as an electron source [139]. The electrons are then collimated into a narrow beam using an electromagnetic coil. The kinetic energy resulting from the electrons transfers heat into the powder bed. In doing so, the negative charge of the powder bed is also increased, requiring helium gas to be released during the melting process in order to dissipate the charge [140]. This feature increases the minimum feature size that the EBM process can produce, enabling the use of larger powder particle sizes compared to other PBF technologies. Similar to SLM, EBM also uses metal and alloyed powders as its main feedstock material [141, 142]. However, only a limited number of metals (e.g., titanium, cobalt chrome, stainless steel, aluminium and copper) are suited for this application, with cobalt chrome and titanium being the most commonly used.

EBM has been widely used in the fabrication of acetabular cups for hip replacement, with more than 60,000 units produced worldwide [143]. Similarly, EBM has shown to be a viable and cost-effective method for producing bespoke hip stems, reducing cost by up to 35% [144]. Owing to the high resolution of EBM, highly porous implants (e.g., hip stems and femoral implants) can be fabricated without compromising their mechanical properties and performance (Figure 7A and 7B) [145]. Due to that, this technology has been suggested as a suitable method for creating titanium-based hip stems loaded with antibiotics, which can be used for the treatment of total hip

arthroplasty postoperative infections [146]. EBM 3D printed mandibular prostheses were also fabricated using titanium (Figure 7C) [147]. The prostheses were designed based on CT scans obtained from patients and have been shown to be mechanically strong, high porous, light in weight and to promote recovery. Likewise, EBM has also been used to fabricate scaffolds for bone regeneration [148], wherein different drug agents have been investigated, including bone morphogenetic proteins (BMP-2) [149], simvastatin [150] (Figure 7D and 7E). In both cases, the drug agents were added to the scaffolds following printing, wherein they adsorbed onto the titanium alloy.

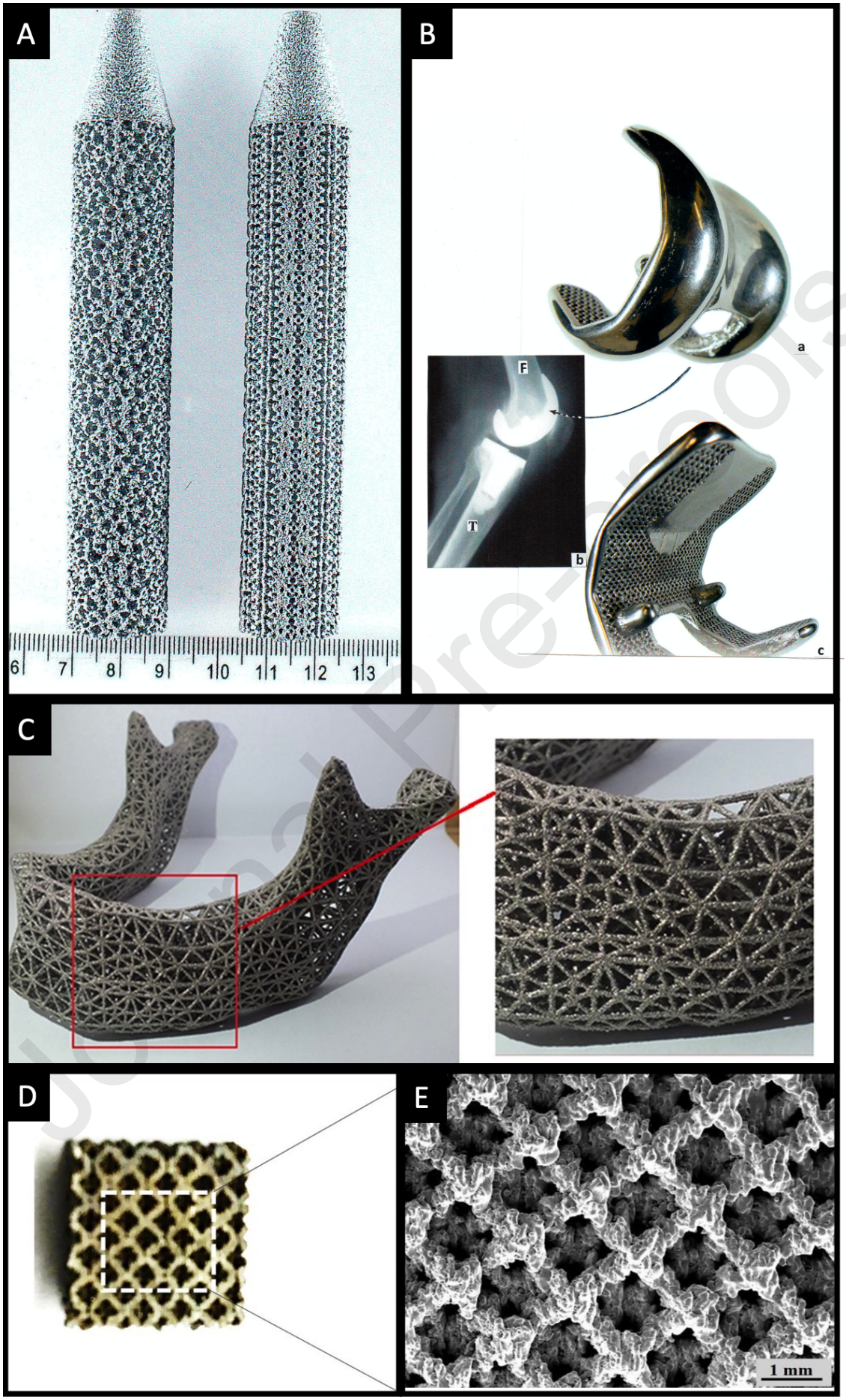
A
6
7
8
9
10
11
12
13
B
a
F
T
b
c
C
D
E
1 mm

Figure 7. (A) Image of EBM 3D printed functionally porous titanium stems. Scale shown in cm. Reprinted with permission from [145]. (B) Image of EBM 3D printed femoral implants used for total knee replacement, fabricated using cobalt–chromium–molybdenum alloy. Reprinted with permission from [145]. (C) Image of an EBM 3D printed mandibular prosthesis fabricated using titanium. Reprinted with permission from [147]. (D) Image and (E) scanning electron micrograph of an EBM 3D printed bone scaffold. Reprinted with permission from [148].

3.4 Multi-jet fusion (MJF)

In MJF, an infrared (IR) lamp acts as the energy source to consolidate powder particles (Figure 1D). MJF normally employs one type of feedstock material, nylon (e.g., PA 12). Unlike the other PBF technologies, MJF requires two additional agents [80]; a fusion agent and a detailing agent. A fusion agent is accurately sprayed onto the printing areas using an ink-jet head. As a result, only the areas covered with the fusion agent will be consolidated, which improves the printing efficiency, accuracy and speed. Unlike binder jetting, the fusion agent does not bind the powder particles alone and instead, requires activation using the energy source for consolidation to be initiated. Thus, the printing process occurs due to the light energy, not the liquid binder. The detailing agent, on the other hand, absorbs heat from the edges of the object, decreasing thermal bleeding (which refers to heat diffusion to adjacent areas) enhancing the printing resolution and accuracy. Compared with SLS, MJF has shown to be more cost-effective, irrespective of the number of parts being produced [72].

Unlike the other PBF technologies, MJF has not yet been explored for drug delivery. This can be mainly attributed to the limited number of materials available for use, and

the requirement for nylon as the base polymer. Instead, MJF has been combined with 3D scanning and imaging techniques to create patient-specific products. This ensures proper fitting and maximises the efficiency of the product. As an example, MJF has been used to create bespoke ankle-foot orthoses for stroke patients, improving their ability to walk [151]. Likewise, MJF 3D printed prosthetic arms were designed for patients with forequarter amputations (Figure 8A and B) [152]. The prosthesis was found to be light in weight, had accurate fitting, was easy to use and could be securely placed. MJF has also been applied for the fabrication of helmets used in the treatment of malignant scalp tumours (Figure 8C and D) [153]. The MJF helmet was made using polyamide 12 (PA-12) and aimed at reducing the air gap between the patient's head and bolus, enabling the delivery of accurate doses of radiation therapy.

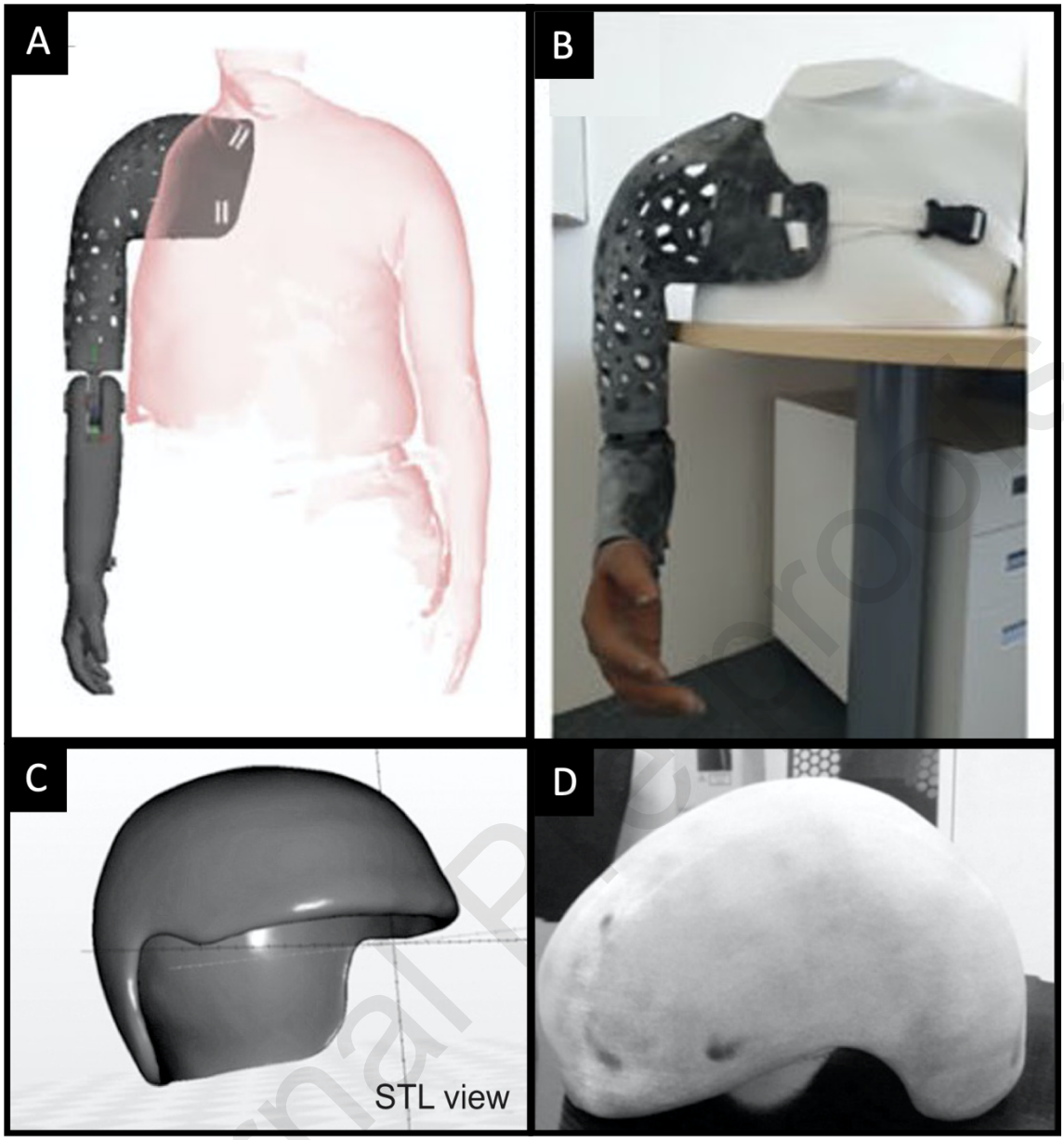

Figure 8. (A) 3D design and (B) image of a MJF 3D printed prosthetic arm for forequarter amputation. Reprinted with permission from [152]. (C) 3D design and (D) image of a MJF 3D printed helmet for cancer therapy. Reprinted with permission from [153].

4 Technical considerations

4.1 Effects of processing parameters

Like other 3D printing technologies, the processing parameters employed during the printing process in PBF can significantly impact the properties of the final 3D object. Therefore, to ensure that the 3D object is printed with optimum characteristics, the processing parameters have to be optimised to meet the requirements of the intended application and properties of the feedstock powder. To do so, it is important to understand how each processing parameter impacts the printing process and its effect on the feed powder [154]. The main processing parameters relating to the PBF technology include (i) printing temperature, (ii) energy source and absorptance, (iii) scanning speed, (iv) scan spacing, (v) particle morphology and (vi) layer thickness, and are summarised in **Table 2** and **Figure 9**.

There are also other parameters that may affect the final outcome of the PBF processes. These include (i) printing orientation (e.g., horizontal, vertical or diagonal), which influences the physical and mechanical characteristics of the final 3D object [155-157]; (ii) building position, which refers to the location at which the printed object is placed on the build plate and can affect the mechanical properties of the 3D object (e.g., middle areas of the build platform retain heat for longer times, causing them to absorb higher energy density); (iii) inert gas (e.g., argon or nitrogen), which is responsible for the removal of condensates from the printing chamber, preventing oxidation from occurring [158]; (iv) dwell time, which is the cooldown time at the beginning and end of each printing layer and as it increases the final geometrical features of the 3D printed object are enhanced [159]; and (v) post-treatment, which includes coating, annealing and surface finishing and influences the tensile strength, surface hardness, dimensional accuracy and precision of the final objects [160-162].

Table 2. A summary of the most important processing parameters involved in PBF 3D printing.

Processing parameter	Description	Classifications/Definitions	Equation(s)	Effect(s)	Reference(s)
Printing temperature	The powder bed temperature is the temperature of the feed powder inside the building platform and is normally regulated using the surface temperature and the chamber temperature.	• **Surface temperature**: the temperature of the superficial layers of the powder inside the build platform. • **Chamber temperature**: the temperature in the printer chamber.	Simple Fox equation: $\frac{1}{T_g} = \frac{W_1}{T_g'} + \frac{W_2}{T_g''}$ W_1 and W_2: weight fractions of each polymer T_g' and T_g'' : Glass transition temperature (T_g) of each individual polymer.	• Controlling the powder bed temperature is essential for inducing the 3D printing process. • The use of heat lowers the amount of energy needed for consolidation, minimising internal stress and thermal deformation.	[160]

Energy source and absorptance	An energy source is needed to induce the consolidation process. The efficiency of a powder in absorbing energy is known as its absorptance and is defined as the ratio of absorbed radiant energy to the incident radiant power.	Energy sources include:
		• Laser beams:
		  ○ Nd:YAG lasers
		  ○ CO_2 lasers
		  ○ CO lasers
		  ○ Diode lasers
		  ○ Fibre lasers
		• Electron beams
		• Infrared lamp
		
		Absorptance depends on:
		• Energy wavelength (λ)
		• Feed powder type
		• Powder morphology
		• Ambient gas within the controlled atmosphere
		• Powder bed temperature
		
		Energy transmittance depends on:
		• Beam power
		• Scanning speed
			$A = 1 - R$
			A: Absorptance
			R: Reflectance
				• Nd:YAG lasers are the oldest, whereas CO_2 lasers are currently the most commonly used. Fibre lasers have a higher laser power density than CO_2 lasers. Diode lasers have a better consistency in melting and heating zones compared to all the other laser types.
				• The wavelength of the beam is one of the few parameters that is intrinsic to the machine and thus, cannot be adjusted.
				• In most cases, as the density of a powder increases, its absorption depth is reduced (Exception are transparent materials). With loose powders, the incident radiation is distributed between the pores and at the surface, increasing the absorptance depth.
					[163-168]

Scanning speed	The rate at which an energy beam travels	The scanning speed is also known as the beam speed.	For lasers:	• The scanning speed can have significant impact on the	[169-173]

	across the powder bed is known as the scanning speed.	Scanning speed controls: • Contact time • Energy transmittance • Printing time	$ED = \frac{P}{V_s \times LT \times h}$ ED: Laser energy density P: Laser power V_s: Laser scanning speed LT: Layer thickness h: Scan spacing	energy density of the powder bed surface. • As the scanning speed is lowered, the contact time between the energy source and powder bed increases and more energy is transmitted to the powder bed. Consequently, more dense objects are produced, and the printing time increases.	
Scan spacing	Scan spacing is the distance travelled between two consecutive scanning vectors.	Scan spacing is also known as the hatch distance or line offset Scan spacing is associated with: • The beam diameter • Energy density. • Printing time.	-	• When the scan space is too large, the interconnections between consecutive layers might not be formed, yielding 3D objects with low mechanical properties. • As the scan spacing is increased, the printing time of each layer is reduced. Whilst this makes the fabrication process longer, it enables the creation of thin and intricate structures. • If the scan spacing is too small, it may result in thermal deformations.	[170, 174, 175]
Layer thickness	Layer thickness is the height of each individual 3D printed layer.	Layer thickness is also known as the slice thickness. Layer thickness depends on: • The 3D printer • Depth by which the build platform is lowered at the start of each layer Layer thickness affects: • Printing resolution • Appearance of the final object • Printing time	-	• As the layer thickness is reduced, the printing resolution is enhanced and the surface of the 3D printed object appears smoother but the printing time increases. • The layer thickness should not fall below the average particle size of the powder.	[160, 164]

Particle morphology	Particle morphology refers to the feed powder's particle size and shape.	Particles should have: • Good flow properties. • Optimum size and shape • Consistency in size and shape Particle size and shape requirements depend upon: • Energy source • Beam power Particle size and shape will determine: • Energy density needed for consolidation • Energy absorption • Flow properties of the feed powder • Mechanical properties of the final object • Porosity of the 3D object	-	• Big particles need more energy for consolidation and bigger empty spaces are left between neighbouring particles, resulting in poor mechanical properties. • Very small particles have high electrostatic charges, causing them to agglomerate and affecting their flow properties. Therefore, resulting in uneven consolidation across the powder bed. • Narrow particle size distribution ensures even energy absorption. • Uneven particle shape results in irregular consolidation and poor particle flow.	[73, 176, 177]

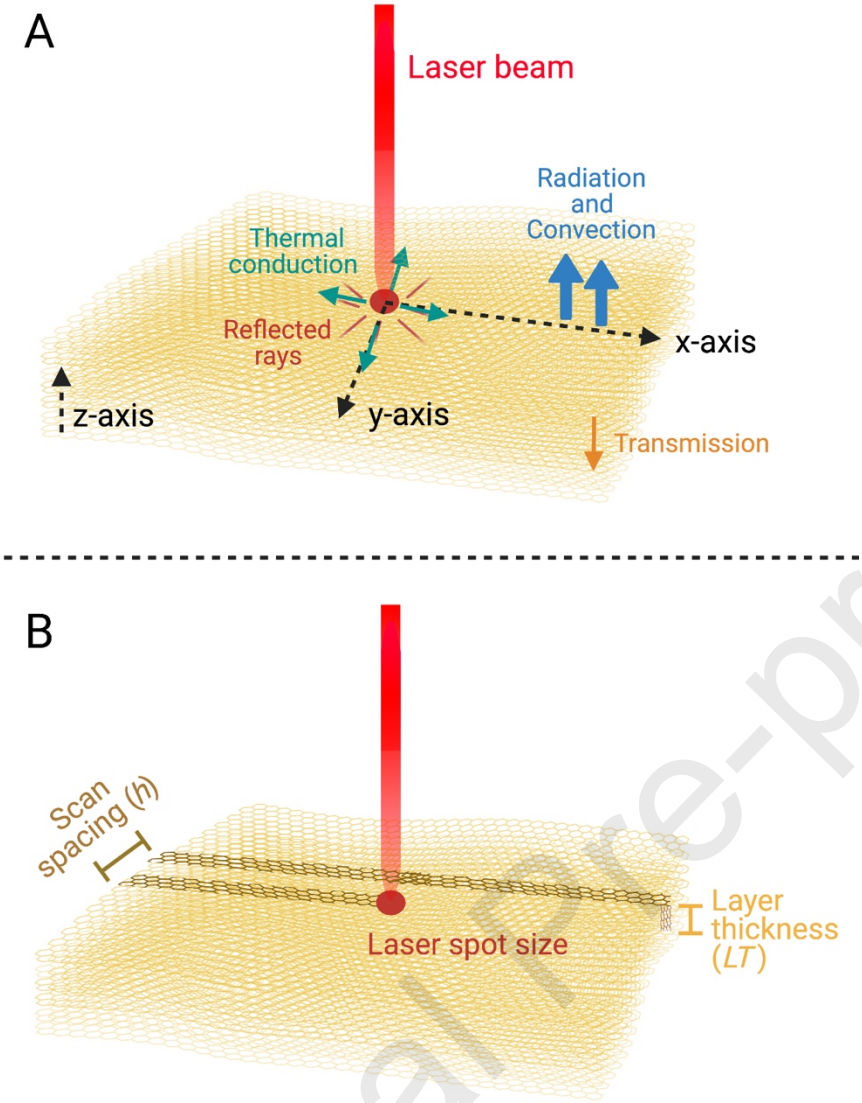

Figure 9. Graphical illustration explaining the (**A**) main events and (**B**) the terms associated with PBF technologies. Create using BioRender.com

By identifying the different processing parameters and their effects, it is possible to integrate advanced technologies, such as artificial intelligence or computer vision, to help in selecting the most optimum printing conditions. In particular, machine learning can be used to train and create a software than can predict the most optimum printing conditions for each formulation [178-180], thus accelerating the printing process and reducing costs and wastage of materials.

4.2 Adapting the technology for healthcare applications

The powder feedstock used in the PBF technologies primarily comprises thermoplastic polymers or metals and alloyed powders. However, commercial materials are mostly unsuited for use within healthcare. This is because these feed powders need to be biocompatible (e.g., generally recognised as safe, GRAS) as per the FDA's certification. As such, conventional powders are typically substituted with pharmaceutical-grade materials with similar properties. In the case of thermoplastic polymers, a wide variety of polymer are available for use, and their selection mainly depends on the desired use (e.g., dosage form and site of action) and the drug release pattern intended. Different biocompatible polymers and metals have been successfully employed for healthcare applications and are summarised in **Table 3**.

Irrespective of its intended application, the selected powder should still meet the printing requirements of the PBF technology. This includes having appropriate powder flow properties and appropriate particle shape and size. To improve the flow properties of the powder, pharmaceutical-grade excipients such as flow enhancers can be added (e.g., lactose monohydrate [100], microcrystalline cellulose [101] and mannitol [99]). To enhance the particle morphology of the PBF feedstock, it can be pre-processed. As an example, to reduce the particle size, the powder can be grinded or milled [181, 182]. To improve the particle shape, spray drying can be used [181, 182]. On the other hand, to obtain an even particle size distribution, it is recommended to sieve the feed powder prior to its use [104]. Some powders may require the addition of an absorptance enhancer. The type of absorptance enhancer suitable for use will depend upon the wavelength of the energy source. As an example, for a diode laser that

operates at a 445 nm wavelength, the addition of a colouring agent (e.g., 3% Candurin Gold Sheen [93], 3% Candurin NXT Ruby Red [183] or 5% charcoal [184]) could significantly improve the absorptance from the laser beam. More recently, it was shown that only 0.1- 0.2% tartrazine lake is needed for use with a 450 nm diode laser [185]. However, it is also possible to print using the drug and polymer alone if the material absorb at the wavelength of the laser, such as in the case of CO_2 lasers (λ = 10.6 μm) [186].

Table 3. Summary of the different biocompatible materials used in PBF 3D printing for healthcare applications.

Type	Material	Drug(s)	Technology(s)	Application(s)	Reference(s)
Thermoplastic polymers	Cellulose acetate	-	SLS	Scaffolds for tissue engineering and drug delivery	[171]
	Starch–cellulose	-	SLS	Scaffolds for tissue engineering and drug delivery	[171]
	Eudragit L100-55	Paracetamol	SLS	Cylindrical, gyroid lattice and bi-layer printlets	[93, 103]
	Eudragit RL	Paracetamol	SLS	Gyroid lattice and bi-layer printlets	[103]
	Ethyl cellulose	Paracetamol, Ibuprofen	SLS	Gyroid lattice and bi-layer printlets and mini-Printlets	[103, 104]
	HAP	-	SLS	Implants for tissue and bone regeneration	[107]
	High density polyethylene	Progesterone, 5-fluorouracil	SLS	Intrauterine devices, tissue and bone regeneration implants	[105, 113]
	HPMC	Paracetamol	SLS	Cylindrical printlets	[97]
	Kollicoat IR	Paracetamol, Ibuprofen, Lopinavir	SLS	Cylindrical printlets and mini-Printlets	[93, 104, 183]
	Kollidon VA64	Ondansetron, Paracetamol, Clindamycin Palmitate Hydrochloride and Diclofenac sodium	SLS	Orally disintegrating printlets	[99-102, 186]
	PCL	5-fluorouracil, Progesterone and Ibuprofen	SLS	Implants for tissue and bone regeneration, multi-reservoir drug delivery systems controlled-release and coronary artery stents	[73, 109, 112, 114, 126, 187-189]
	Polyethylene oxide	Paracetamol	SLS	Gyroid lattice and bi-layer printlets	[103]
	Polypropylene	-	SLS	Mandible implants with an embedded drug delivery system	[106]
	PLA	-	SLS	Implants for tissue and bone regeneration	[107]
	PLLA	Paracetamol	SLS, SLM	Controlled-release printlets and coronary artery stents	[73, 126]
Metals and alloyed powders	Cobalt–chromium–	-	SLM	Implants for bone regeneration	[120]

molybdenum alloy				
Titanium	Vancomycin, Paracetamol, Ciprofloxacin, silver ions, morphogenetic proteins (BMP-2), Simvastatin, Penicillin, Dexamethasone, Streptomycin and Minocycline	SLM, EBM, DMLS	Implants and scaffolds for bone regeneration, implants with controllable drug release kinetics, orthopaedic implants and hip stems	[120, 123-125, 129, 130, 135, 146, 148-150]

HAP, hydroxyapatite; HPMC, hydroxypropyl methylcellulose; IR, instant release; PCL, polycaprolactone; PLA, poly(lactic acid); PLLA, poly-L-lactide; SLS, selective laser sintering; SLM, selective laser melting; DMLS, direct metal laser sintering; EBM, electron beam melting.

5 Challenges, solutions and future outlook

5.1 Powder amount and stability

Typically, the PBF printing process requires the use of large amounts of powder to ensure consistent layer height and suitable flow of powders during printing. However, this may not be always feasible, especially in the case of drug available in limited quantities or expensive drug substances [190]. Additionally, different 3D printers will require different volumes of powder, making the requirements variable depending on which system is being used.

Despite the possibility of reusing unconsolidated feed powders with PBF, the powders can only be recycled for a few numbers of times. This is because the drug substance may be chemically unstable or undergo physical changes during the printing process [191]. Similarly, the polymer or metal particles may undergo changes in size, shape and/or surface properties when re-used, affecting their printability [192, 193]. Due to that, it is necessary to optimise the printing process to avoid any unnecessary waste of drug substances or the incurring of additional costs. A proper solution to this would include modifying the printers to include powder dispensers that can precisely deposit the amount of powder needed for printing onto the printing platform. This would help in reducing the amount of powder used per printing job and avoid post-processing.

5.2 Printing speed and variability in finished products

Although PBF technologies are generally faster than some of the other 3D printing technologies (e.g., extrusion-based technologies), they are relatively slower than some of the conventional pharmaceutical production methods (e.g., tabletting). Furthermore, the PBF technology may require the use of additional processes when

post-treatment of the printed object is needed (e.g., sieving and brushing Printlets), thus prolonging the overall production time and imparting extra expenses [194]. In this regard, the use of automatic sieves (i.e., for retrieving parts from the printing platform) and closed-loop powder controllers (i.e., for recycling unsintered powder from the building platform back to the reservoir platform/hopper), multi-layer printing (i.e., the 3D printing of more than one layer at a time), multi-powder hoppers (i.e., hoppers for multiple, different feedstock materials), multi-process printers (i.e., printers that integrate other complementary processes within the same print job) and multi-laser systems (i.e., printers that operate using more than one laser beam within the same print job) have shown to improve the efficiency of PBF 3D printing by increasing output whilst reducing expenditure [195, 196].

Like other 3D printing technologies, PBF suffers from issues relating to printing variability. As an example, it was previously shown that heat transfer could differ depending on the printing location on the build platform [80, 197]. Hence, resulting in 3D printed parts with different mechanical properties and porosities. Moreover, in some cases, thermal expansion and contraction could lead to the warping (i.e., bending or curling) of the printed object [69, 198]. Therefore, it is necessary to ensure that the powder bed and printing chamber are sufficiently and evenly heated throughout the printing process to provide an adequate amount of heat for successful printing.

5.3 Regulatory challenges

In 2017, a guidance on the “technical considerations for medical devices manufactured using additive manufacturing” was issued by the FDA, highlighting the main factors to

be considered when designing and manufacturing 3D printed products [199]. However, the guidance does not cover 3D printed drug products or biomedical implants. Thus, at the moment there is not a specific guidance to be followed. Hence, it is crucial to define a set of requirements that are specific for 3D printed drug products, wherein all technical aspects (e.g., feed materials, 3D printing process and 3D printed product validation) should be covered [200].

At present, not all commercial PBF 3D printers are made for use within healthcare and do not comply with Good Manufacturing Practice (GMP) specifications for drug products, so therefore are unsuitable for use in the production of drug-laden products. This calls for the need to develop new PBF platforms that are specific to healthcare use for drug products and conform with GMP requirements. Like any other new equipment, developing a PBF 3D printer causes technical and logistical challenges. As an example, the 3D printer may produce inconsistent products or drug doses. Thus, it is necessary to optimise the process to ensure dose uniformity and end-product consistency. To do so, in-process quality control (QC) methods need to be implemented.

To facilitate this, rapid ‘point-and-shoot’ process analytical technologies (PAT) based on portable near infrared (NIR) spectrometry or Raman confocal microscopy have been suggested as viable, non-destructive approaches for the verification of drug doses [201-204]. This method has been shown to be effective on SLS Printlets with different geometries [205]. Other information, including the solid state of the drug, its polymorphism, interactions, stability, moisture content, purity, breaking force and disintegration properties, can also be derived [206-209]. These approaches can also

be applied for dose verification in Printlets with multiple drug agents, wherein the validated calibration models are generated using partial least squares regression [210]. Alternatively, NIR hyperspectral imaging can be utilised to quantify drugs and analyse their spatial distribution within Printlets [211]. Geometric and printing accuracy monitoring can also be achieved via the use of imaging techniques and artificial vision, wherein thermal imaging could be used to predict the mechanical properties of the Printlets [209, 212, 213].

Finally, although biocompatible feed materials (e.g., thermoplastic polymers, drug substances and metals) are suitable for use with the PBF technologies, they have not been approved for such uses. In particular, the PBF processes involve the use of heat and energy sources, both of which may induce chemical changes in the drug product and/or excipients. Moreover, different printing systems and conditions will have variable effects. Thus, approval for using these excipients with the PBF 3D printing technologies should be obtained taking these aspects into consideration.

Despite the absence of FDA-approved drug-loaded products made using PBF, there is an increased interest in this technology. This particularly due to its ability to produce solid amorphous dispersions, which aid in improving the solubility of poorly soluble drugs. Moreover, PBF offers flexibility in altering the dose, shape and release characteristics of drug delivery systems, making it a useful tool in early preclinical and clinical studies. As an example, Merck has recently announced that it will be using SLS 3D printing to fabricate formulations for clinical studies in a more efficient and simple manner [214]. The ability to produce multiple drug-laden iterations in a short time frame enables the rapid customisation of the dosage forms based on the progress

and requirements of the study design [215]. Given that it currently takes a drug product 10 to 15 years to reach the market [216], such an approach can have significant advantages in expediting drug development whilst reducing expenditure.

6 Conclusion

The Powder Bed Fusion (PBF) technologies have shown great potential as versatile manufacturing tools for the fabrication of novel drug-laden products for various healthcare applications. Due to the absence of need for support materials, PBF can be used to create dosage forms with unique structural and functional designs that are typically complex or impossible to produce using conventional processes or other printing technologies. By combining it with imaging and 3D scanning technologies, patient-specific drug delivery systems can be designed for targeted therapy. This enables the creation of dosage forms and medical devices with optimum characteristics and fitting, enhancing the efficiency of treatment and improving healthcare outcomes. Compared with other 3D printing technologies, the adoption of PBF for mass production within healthcare may be realised more rapidly because of its similarity with traditional production methods and ability to be scaled up. Whether the PBF technologies are eventually embraced within healthcare or not remains unknown, though the rapidly evolving research and preliminary outcomes would suggest in favour.

Declarations of interest: none

Acknowledgments

The graphical abstract was created using biorender.com

References

[1] S.J. Trenfield, A. Awad, C.M. Madla, G.B. Hatton, J. Firth, A. Goyanes, S. Gaisford, A.W. Basit, Shaping the future: recent advances of 3D printing in drug delivery and healthcare, EXPERT OPIN DRUG DEL, 16 (2019) 1081-1094.

[2] W.K. Hsiao, B. Lorber, H. Reitsamer, J. Khinast, 3D printing of oral drugs: a new reality or hype?, Expert Opin Drug Deliv, 15 (2018) 1-4.

[3] K.R. Ryan, M.P. Down, C.E. Banks, Future of additive manufacturing: Overview of 4D and 3D printed smart and advanced materials and their applications, Chemical Engineering Journal, 403 (2021) 126162.

[4] S. Beg, W.H. Almalki, A. Malik, M. Farhan, M. Aatif, K.S. Alharbi, N.K. Alruwaili, M. Alrobaian, M. Tarique, M. Rahman, 3D printing for drug delivery and biomedical applications, Drug Discov. Today, 25 (2020) 1668-1681.

[5] K.P.A. Kumar, M. Pumera, 3D-Printing to Mitigate COVID-19 Pandemic, Adv Funct Mater, (2021) 2100450.

[6] O. Jennotte, N. Koch, A. Lechanteur, B. Evrard, Three-dimensional printing technology as a promising tool in bioavailability enhancement of poorly water-soluble molecules: A review, Int J Pharm, 580 (2020) 119200.

[7] S. Mukhopadhyay, R. Poojary, A review on 3D printing: Advancement in healthcare technology, 2018 Advances in Science and Engineering Technology International Conferences (ASET), 2018, pp. 1-5.

[8] W. Jamróz, J. Szafraniec, M. Kurek, R. Jachowicz, 3D Printing in Pharmaceutical and Medical Applications – Recent Achievements and Challenges, Pharmaceutical Research, 35 (2018) 176.

[9] S.J. Trenfield, A. Awad, A. Goyanes, S. Gaisford, A.W. Basit, 3D Printing Pharmaceuticals: Drug Development to Frontline Care, Trends Pharmacol. Sci., 39 (2018) 440-451.

[10] J.J. Ong, A. Awad, A. Martorana, S. Gaisford, E. Stoyanov, A.W. Basit, A. Goyanes, 3D printed opioid medicines with alcohol-resistant and abuse-deterrent properties, Int J Pharm, 579 (2020) 119169.

[11] N.A. Elkasabgy, A.A. Mahmoud, A. Maged, 3D printing: An appealing route for customized drug delivery systems, Int J Pharm, (2020) 119732.

[12] ASTM International, Standard Guidelines for Design for Additive Manufacturing, Section 3: TerminologyWest Conshohocken, PA, 2016.

[13] M. Pandey, H. Choudhury, J.L.C. Fern, A.T.K. Kee, J. Kou, J.L.J. Jing, H.C. Her, H.S. Yong, H.C. Ming, S.K. Bhattamisra, 3D printing for oral drug delivery: a new tool to customize drug delivery, Drug Delivery and Translational Research, 10 (2020) 986-1001.

[14] D. Tan, A. Nokhodchi, M. Maniruzzaman, 3D and 4D printing technologies: innovative process engineering and smart additive manufacturing, 3D and 4D Printing in Biomedical Applications: Process Engineering and Additive Manufacturing, (2019) 25-52.

[15] C.I. Gioumouxouzis, C. Karavasili, D.G. Fatouros, Recent advances in pharmaceutical dosage forms and devices using additive manufacturing technologies, Drug Discov. Today, 24 (2019) 636-643.

[16] M.M. Prabhakar, A. Saravanan, A.H. Lenin, K. Mayandi, P.S. Ramalingam, A short review on 3D printing methods, process parameters and materials, Materials Today: Proceedings, (2020).

[17] S. Jacob, A.B. Nair, V. Patel, J. Shah, 3D Printing Technologies: Recent Development and Emerging Applications in Various Drug Delivery Systems, AAPS PharmSciTech, 21 (2020) 1-16.

[18] I. Seoane-Viaño, P. Januskaite, C. Alvarez-Lorenzo, A.W. Basit, A. Goyanes, Semi-solid extrusion 3D printing in drug delivery and biomedicine: Personalised solutions for healthcare challenges, Journal of Controlled Release, (2021).

[19] A.W. Basit, S. Gaisford, 3D Printing of Pharmaceuticals, 1 ed., Springer International Publishing2018.

[20] G. Chen, X. Yihua, P. Kwok, L. Kang, Pharmaceutical Applications of 3D Printing, Additive Manufacturing, 34 (2020) 101209.

[21] O. Bongomin, A. Yemane, B. Kembabazi, C. Malanda, M.C. Mwape, N.S. Mpofu, D. Tigalana, Industry 4.0 Disruption and Its Neologisms in Major Industrial Sectors: A State of the Art, Journal of Engineering, 2020 (2020).

[22] R.D.P. Reddy, V. Sharma, Additive manufacturing in drug delivery applications: A review, Int J Pharm, 589 (2020) 119820.

[23] R.T. Ponni, M. Swamivelmanickam, S. Sivakrishnan, 3D Printing in Pharmaceutical Technology–A Review, International Journal of Pharmaceutical Investigation, 10 (2020) 8-12.

[24] R. Fernández-García, M. Prada, F. Bolás-Fernández, M.P. Ballesteros, D.R. Serrano, Oral fixed-dose combination pharmaceutical products: Industrial manufacturing versus personalized 3D printing, Pharmaceutical research, 37 (2020) 1-22.

[25] M. Czölderová, M. Behúl, J. Filip, P. Zajíček, R. Grabic, A. Vojs-Staňová, M. Gál, K. Kerekeš, J. Híveš, J. Ryba, M. Rybanská, P. Brandeburová, T. Mackuľak, 3D printed polyvinyl alcohol ferrate(VI) capsules: Effective means for the removal of pharmaceuticals and illicit drugs from wastewater, Chemical Engineering Journal, 349 (2018) 269-275.

[26] M. Elbadawi, J.J. Ong, T.D. Pollard, S. Gaisford, A.W. Basit, Additive Manufacturable Materials for Electrochemical Biosensor Electrodes, Adv Funct Mater, 31 (2021) 2006407.

[27] M. Cui, H. Pan, Y. Su, D. Fang, S. Qiao, P. Ding, W. Pan, Opportunities and challenges of three-dimensional printing technology in pharmaceutical formulation development, Acta Pharmaceutica Sinica B, (2021) In Press.

[28] I. Seoane-Viaño, J.S. Trenfield, A.W. Basit, A. Goyanes, Translating 3D printed pharmaceuticals: from hype to real-world clinical applications, Advanced Drug Delivery Reviews, (2021) In Press.

[29] P. Januskaite, X. Xu, S.R. Ranmal, S. Gaisford, A.W. Basit, C. Tuleu, A. Goyanes, I Spy with My Little Eye: A Paediatric Visual Preferences Survey of 3D Printed Tablets, Pharmaceutics, 12 (2020) 1100.

[30] K. Vithani, A. Goyanes, V. Jannin, A.W. Basit, S. Gaisford, B.J. Boyd, An Overview of 3D Printing Technologies for Soft Materials and Potential Opportunities for Lipid-based Drug Delivery Systems, Pharmaceutical Research, 36 (2018) 4.

[31] O.S. Fenton, M. Paolini, J.L. Andresen, F.J. Müller, R. Langer, Outlooks on Three-Dimensional Printing for Ocular Biomaterials Research, Journal of Ocular Pharmacology and Therapeutics, 36 (2019) 7-17.

[32] A.Z. Wang, Personalized drug tablets with 3D printing, Science Translational Medicine, 7 (2015) 312ec191.

[33] B.C. Pereira, A. Isreb, M. Isreb, R.T. Forbes, E.F. Oga, M.A. Alhnan, Additive Manufacturing of a Point-of-Care “Polypill:” Fabrication of Concept Capsules of Complex Geometry with Bespoke Release against Cardiovascular Disease, Advanced Healthcare Materials, 9 (2020) 2000236.

[34] M. Vivero-Lopez, X. Xu, A. Muras, A. Otero, A. Concheiro, S. Gaisford, A.W. Basit, C. Alvarez-Lorenzo, A. Goyanes, Anti-biofilm multi drug-loaded 3D printed hearing aids, Materials Science and Engineering: C, (2020) 111606.

[35] A.Q. Vo, J. Zhang, D. Nyavanandi, S. Bandari, M.A. Repka, Hot melt extrusion paired fused deposition modeling 3D printing to develop hydroxypropyl cellulose based floating tablets of cinnarizine, Carbohydrate Polymers, 246 (2020) 116519.

[36] J. dos Santos, R.S. de Oliveira, T.V. de Oliveira, M.C. Velho, M.V. Konrad, G.S. da Silva, M. Deon, R.C.R. Beck, 3D Printing and Nanotechnology: A Multiscale Alliance in Personalized Medicine, Adv Funct Mater, (2021) 2009691.

[37] A. Awad, S. Gaisford, A.W. Basit, Fused Deposition Modelling: Advances in Engineering and Medicine, in: A.W. Basit, S. Gaisford (Eds.) 3D Printing of Pharmaceuticals, Springer International Publishing, Cham, 2018, pp. 107-132.

[38] C. Yu, J. Schimelman, P. Wang, K.L. Miller, X. Ma, S. You, J. Guan, B. Sun, W. Zhu, S. Chen, Photopolymerizable Biomaterials and Light-Based 3D Printing Strategies for Biomedical Applications, Chemical Reviews, 120 (2020) 10695–10743.

[39] A. Melocchi, M. Uboldi, A. Maroni, A. Foppoli, L. Palugan, L. Zema, A. Gazzaniga, 3D printing by fused deposition modeling of single- and multi-

compartment hollow systems for oral delivery – A review, Int. J. Pharm., 579 (2020) 119155.

[40] X. Zhu, H. Li, L. Huang, M. Zhang, W. Fan, L. Cui, 3D printing promotes the development of drugs, Biomedicine & Pharmacotherapy, 131 (2020) 110644.

[41] M. Wallis, Z. Al-Dulimi, D.K. Tan, M. Maniruzzaman, A. Nokhodchi, 3D printing for enhanced drug delivery: current state-of-the-art and challenges, Drug Development and Industrial Pharmacy, 46 (2020) 1385-1401.

[42] A. Mohammed, A. Elshaer, P. Sareh, M. Elsayed, H. Hassanin, Additive manufacturing technologies for drug delivery applications, Int J Pharm, 580 (2020) 119245.

[43] K. Liang, D. Brambilla, J.-C. Leroux, Is 3D Printing of Pharmaceuticals a Disruptor or Enabler?, Advanced Materials, 31 (2019) 1805680.

[44] X. Xu, P. Robles-Martinez, C.M. Madla, F. Joubert, A. Goyanes, A.W. Basit, S. Gaisford, Stereolithography (SLA) 3D printing of an antihypertensive polyprintlet: Case study of an unexpected photopolymer-drug reaction, Additive Manufacturing, 33 (2020) 101071.

[45] Y.L. Kong, X. Zou, C.A. McCandler, A.R. Kirtane, S. Ning, J. Zhou, A. Abid, M. Jafari, J. Rogner, D. Minahan, J.E. Collins, S. McDonnell, C. Cleveland, T. Bensel, S. Tamang, G. Arrick, A. Gimbel, T. Hua, U. Ghosh, V. Soares, N. Wang, A. Wahane, A. Hayward, S. Zhang, B.R. Smith, R. Langer, G. Traverso, 3D-Printed Gastric Resident Electronics, Advanced Materials Technologies, 4 (2019) 1800490.

[46] Aprecia Pharmaceuticals, Our story, 2018. https://www.aprecia.com/about.

[47] C.I. Gioumouxouzis, E. Tzimtzimis, O.L. Katsamenis, A. Dourou, C. Markopoulou, N. Bouropoulos, D. Tzetzis, D.G. Fatouros, Fabrication of an osmotic 3D printed solid dosage form for controlled release of active pharmaceutical ingredients, Eur. J. Pharm. Sci., 143 (2020) 105176.

[48] L.-D. Iftimi, M. Edinger, D. Bar-Shalom, J. Rantanen, N. Genina, Edible solid foams as porous substrates for inkjet-printable pharmaceuticals, European Journal of Pharmaceutics and Biopharmaceutics, 136 (2019) 38-47.

[49] R. Thakkar, A.R. Pillai, J. Zhang, Y. Zhang, V. Kulkarni, M. Maniruzzaman, Novel On-Demand 3-Dimensional (3-D) Printed Tablets Using Fill Density as an Effective Release-Controlling Tool, Polymers, 12 (2020) 1872.

[50] S.J. Trenfield, H. Xian Tan, A. Awad, A. Buanz, S. Gaisford, A.W. Basit, A. Goyanes, Track-and-trace: Novel anti-counterfeit measures for 3D printed personalized drug products using smart material inks, Int J Pharm, 567 (2019) 118443.

[51] N. Reddy Dumpa, S. Bandari, M. A. Repka, Novel Gastroretentive Floating Pulsatile Drug Delivery System Produced via Hot-Melt Extrusion and Fused Deposition Modeling 3D Printing, Pharmaceutics, 12 (2020) 52.

[52] A.J. Capel, R.P. Rimington, M.P. Lewis, S.D.R. Christie, 3D printing for chemical, pharmaceutical and biological applications, Nature Reviews Chemistry, 2 (2018) 422-436.

[53] E.R. Ghomi, F. Khosravi, R.E. Neisiany, S. Singh, S. Ramakrishna, Future of Additive Manufacturing in Healthcare, Current Opinion in Biomedical Engineering, (2020) 100255.

[54] S.K. Eshkalak, E.R. Ghomi, Y. Dai, D. Choudhury, S. Ramakrishna, The role of three-dimensional printing in healthcare and medicine, Materials & Design, (2020) 108940.

[55] O.L. Okafor-Muo, H. Hassanin, R. Kayyali, A. ElShaer, 3D Printing of Solid Oral Dosage Forms: Numerous Challenges With Unique Opportunities, J. Pharm. Sci., 109 (2020) 3535-3550.

[56] O. Jennotte, N. Koch, A. Lechanteur, B. Evrard, Three-dimensional printing technology as a promising tool in bioavailability enhancement of poorly water-soluble molecules: a review, Int J Pharm, (2020) 119200.

[57] C.A. Chatham, T.E. Long, C.B. Williams, A review of the process physics and material screening methods for polymer powder bed fusion additive manufacturing, Progress in Polymer Science, 93 (2019) 68-95.

[58] M.S. Hossain, J.A. Gonzalez, R.M. Hernandez, M.A.I. Shuvo, J. Mireles, A. Choudhuri, Y. Lin, R.B. Wicker, Fabrication of smart parts using powder bed fusion additive manufacturing technology, Additive Manufacturing, 10 (2016) 58-66.

[59] J. Williams, P. Revington, Novel use of an aerospace selective laser sintering machine for rapid prototyping of an orbital blowout fracture, International journal of oral and maxillofacial surgery, 39 (2010) 182-184.

[60] T. Hettesheimer, S. Hirzel, H.B. Roß, Energy savings through additive manufacturing: an analysis of selective laser sintering for automotive and aircraft components, Energy Efficiency, 11 (2018) 1227-1245.

[61] M. George, K.R. Aroom, H.G. Hawes, B.S. Gill, J. Love, 3D printed surgical instruments: the design and fabrication process, World journal of surgery, 41 (2017) 314-319.

[62] G.d.A. Di Giacomo, P.R. Cury, A.M. da Silva, J.V. da Silva, S.A. Ajzen, A selective laser sintering prototype guide used to fabricate immediate interim fixed complete arch prostheses in flapless dental implant surgery: Technique description and clinical results, The Journal of prosthetic dentistry, 116 (2016) 874-879.

[63] M. Revilla-León, M. Özcan, Additive Manufacturing Technologies Used for 3D Metal Printing in Dentistry, Current Oral Health Reports, 4 (2017) 201-208.

[64] I. Theodorakos, F. Zacharatos, R. Geremia, D. Karnakis, I. Zergioti, Selective laser sintering of Ag nanoparticles ink for applications in flexible electronics, Applied surface science, 336 (2015) 157-162.

[65] D. King, T. Tansey, Rapid tooling: selective laser sintering injection tooling, Journal of Materials Processing Technology, 132 (2003) 42-48.

[66] Z. Jiba, W.W. Focke, L. Kalombo, M.J. Madito, Coating processes towards selective laser sintering of energetic material composites, Defence Technology, (2019).

[67] A. Awad, F. Fina, A. Goyanes, S. Gaisford, A.W. Basit, 3D printing: Principles and pharmaceutical applications of selective laser sintering, Int J Pharm, 586 (2020) 119594.

[68] L.M. Ricles, J.C. Coburn, M. Di Prima, S.S. Oh, Regulating 3D-printed medical products, Science Translational Medicine, 10 (2018) eaan6521.

[69] I. Gibson, D. Rosen, B. Stucker, Powder Bed Fusion Processes, in: I. Gibson, D. Rosen, B. Stucker (Eds.) Additive Manufacturing Technologies: 3D Printing, Rapid Prototyping, and Direct Digital Manufacturing, Springer New York, New York, NY, 2015, pp. 107-145.

[70] R. Goodridge, S. Ziegelmeier, 7 - Powder bed fusion of polymers, in: M. Brandt (Ed.) Laser Additive Manufacturing, Woodhead Publishing2017, pp. 181-204.

[71] T.G. Spears, S.A. Gold, In-process sensing in selective laser melting (SLM) additive manufacturing, Integrating Materials and Manufacturing Innovation, 5 (2016) 16-40.

[72] A.B. Varotsis, HP MJF vs. SLS: A 3D printing technology comparison, 2020. https://www.3dhubs.com/knowledge-base/hp-mjf-vs-sls-3d-printing-technology-comparison/.

[73] K.F. Leong, C.K. Chua, W.S. Gui, Verani, Building Porous Biopolymeric Microstructures for Controlled Drug Delivery Devices Using Selective Laser Sintering, The International Journal of Advanced Manufacturing Technology, 31 (2006) 483-489.

[74] N. K., The different SLS 3D printers on the market, 2020. https://www.3dnatives.com/en/different-sls-3d-printers-220320184/.

[75] L.E. Murr, E. Martinez, K.N. Amato, S.M. Gaytan, J. Hernandez, D.A. Ramirez, P.W. Shindo, F. Medina, R.B. Wicker, Fabrication of Metal and Alloy Components by Additive Manufacturing: Examples of 3D Materials Science, Journal of Materials Research and Technology, 1 (2012) 42-54.

[76] ForeRunner3D, How does the HP Multi Jet Fusion (also known as MJF or HP 3D printing) work:, 2020. https://forerunner3d.com/hp-multi-jet-fusion-mjf-3d-printing/.

[77] Hp, HP Jet Fusion 540 3D Printer, 2020. https://h20195.www2.hp.com/v2/getpdf.aspx/4AA7-1970ENA.pdf.

[78] Hp, Technical Guideline for Material Development with HP 3D Open Materials Platform, 2018. https://www8.hp.com/h20195/v2/GetPDF.aspx/4AA6-8315ENW.pdf.

[79] P.K. Gokuldoss, S. Kolla, J. Eckert, Additive Manufacturing Processes: Selective Laser Melting, Electron Beam Melting and Binder Jetting—Selection Guidelines, Materials, 10 (2017) 672.

[80] F. Sillani, R.G. Kleijnen, M. Vetterli, M. Schmid, K. Wegener, Selective laser sintering and multi jet fusion: Process-induced modification of the raw materials and analyses of parts performance, Additive Manufacturing, 27 (2019) 32-41.

[81] R. Singh, A. Gupta, O. Tripathi, S. Srivastava, B. Singh, A. Awasthi, S.K. Rajput, P. Sonia, P. Singhal, K.K. Saxena, Powder bed fusion process in additive manufacturing: An overview, Materials Today: Proceedings, 26 (2020) 3058-3070.

[82] S. Hou, S. Qi, D.A. Hutt, J.R. Tyrer, M. Mu, Z. Zhou, Three dimensional printed electronic devices realised by selective laser melting of copper/high-density-polyethylene powder mixtures, Journal of Materials Processing Technology, 254 (2018) 310-324.

[83] P. Rokicki, B. Kozik, G. Budzik, T. Dziubek, J. Bernaczek, L. Przeszlowski, O. Markowska, B. Sobolewski, A. Rzucidlo, Manufacturing of aircraft engine transmission gear with SLS (DMLS) method, Aircraft Engineering and Aerospace Technology: An International Journal, 88 (2016) 397-403.

[84] N. Sudarmadji, J. Tan, K. Leong, C. Chua, Y. Loh, Investigation of the mechanical properties and porosity relationships in selective laser-sintered polyhedral for functionally graded scaffolds, Acta biomaterialia, 7 (2011) 530-537.

[85] A. Nazir, M. Ali, C.-H. Hsieh, J.-Y. Jeng, Investigation of stiffness and energy absorption of variable dimension helical springs fabricated using multijet fusion technology, The International Journal of Advanced Manufacturing Technology, 110 (2020) 2591-2602.

[86] J.-P. Kruth, P. Mercelis, J. Van Vaerenbergh, L. Froyen, M. Rombouts, Advances in selective laser sintering, Proceedings of the 1st International Conference on Advanced Research in Virtual and Rapid Prototyping, 2003, pp. 59-70.

[87] F. Fina, S. Gaisford, A.W. Basit, Powder bed fusion: the working process, current applications and opportunities, in: A.W. Basit, S. Gaisford (Eds.) 3D Printing of Pharmaceuticals, Springer International Publishing2018, pp. 81-105.

[88] J.J. Beaman, C.R. Deckard, Selective laser sintering with assisted powder handling, Google Patents, U.S. Patent 4,938,816, 1990.

[89] M.A. Alhnan, T.C. Okwuosa, M. Sadia, K.W. Wan, W. Ahmed, B. Arafat, Emergence of 3D Printed Dosage Forms: Opportunities and Challenges, Pharm Res, 33 (2016) 1817-1832.

[90] K. Low, K. Leong, C. Chua, Z. Du, C. Cheah, Characterization of SLS parts for drug delivery devices, Rapid Prototyping Journal, 7 (2001) 262-268.

[91] C.M. Cheah, K.F. Leong, C.K. Chua, K.H. Low, H.S. Quek, Characterization of microfeatures in selective laser sintered drug delivery devices, Proc Inst Mech Eng H, 216 (2002) 369-383.

[92] K.F. Leong, F.E. Wiria, C.K. Chua, S.H. Li, Characterization of a poly-epsilon-caprolactone polymeric drug delivery device built by selective laser sintering, Bio-medical materials and engineering, 17 (2007) 147-157.

[93] F. Fina, A. Goyanes, S. Gaisford, A.W. Basit, Selective laser sintering (SLS) 3D printing of medicines, Int J Pharm, 529 (2017) 285-293.

[94] K.F. Leong, C.M. Cheah, C.K. Chua, Solid freeform fabrication of three-dimensional scaffolds for engineering replacement tissues and organs, Biomaterials, 24 (2003) 2363-2378.

[95] A. Awad, S.J. Trenfield, A. Goyanes, S. Gaisford, A.W. Basit, Reshaping drug development using 3D printing, Drug Discov. Today, 23 (2018) 1547-1555.

[96] N. Hopkinson, P. Dicknes, Analysis of rapid manufacturing—using layer manufacturing processes for production, Proceedings of the Institution of Mechanical Engineers, Part C: Journal of Mechanical Engineering Science, 217 (2003) 31-39.

[97] F. Fina, C.M. Madla, A. Goyanes, J. Zhang, S. Gaisford, A.W. Basit, Fabricating 3D printed orally disintegrating printlets using selective laser sintering, Int J Pharm, 541 (2018) 101-107.

[98] D.A. Davis, R. Thakkar, Y. Su, R.O. Williams, M. Maniruzzaman, Selective Laser Sintering 3-Dimensional Printing as a Single Step Process to Prepare Amorphous Solid Dispersion Dosage Forms for Improved Solubility and Dissolution rate, J. Pharm. Sci., 110 (2020) 1432-1443.

[99] N. Allahham, F. Fina, C. Marcuta, L. Kraschew, W. Mohr, S. Gaisford, A.W. Basit, A. Goyanes, Selective Laser Sintering 3D Printing of Orally Disintegrating Printlets Containing Ondansetron, Pharmaceutics, 12 (2020) 110.

[100] S.F. Barakh Ali, E.M. Mohamed, T. Ozkan, M.A. Kuttolamadom, M.A. Khan, A. Asadi, Z. Rahman, Understanding the effects of formulation and process variables on the printlets quality manufactured by selective laser sintering 3D printing, Int J Pharm, 570 (2019) 118651.

[101] E.M. Mohamed, S.F. Barakh Ali, Z. Rahman, S. Dharani, T. Ozkan, M.A. Kuttolamadom, M.A. Khan, Formulation Optimization of Selective Laser Sintering 3D-Printed Tablets of Clindamycin Palmitate Hydrochloride by Response Surface Methodology, AAPS PharmSciTech, 21 (2020) 232.

[102] A. Awad, A. Yao, J.S. Trenfield, A. Goyanes, S. Gaisford, W.A. Basit, 3D Printed Tablets (Printlets) with Braille and Moon Patterns for Visually Impaired Patients, Pharmaceutics, 12 (2020) 172.

[103] F. Fina, A. Goyanes, C.M. Madla, A. Awad, S.J. Trenfield, J.M. Kuek, P. Patel, S. Gaisford, A.W. Basit, 3D printing of drug-loaded gyroid lattices using selective laser sintering, Int J Pharm, 547 (2018) 44-52.

[104] A. Awad, F. Fina, J.S. Trenfield, P. Patel, A. Goyanes, S. Gaisford, W.A. Basit, 3D Printed Pellets (Miniprintlets): A Novel, Multi-Drug, Controlled Release Platform Technology, Pharmaceutics, 11 (2019) 148.

[105] G. Salmoria, F. Vieira, E. Muenz, I. Gindri, M. Marques, L. Kanis, Additive Manufacturing of PE/fluorouracil/progesterone intrauterine device for endometrial and ovarian cancer treatments, Polymer Testing, 71 (2018) 312-317.

[106] J.S. Akmal, M. Salmi, A. Mäkitie, R. Björkstrand, J. Partanen, Implementation of industrial additive manufacturing: intelligent implants and drug delivery systems, J Funct Biomater, 9 (2018) 41.

[107] D. Yan, B. Zeng, Y. Han, H. Dai, J. Liu, Y. Sun, F. Li, Preparation and laser powder bed fusion of composite microspheres consisting of poly(lactic acid) and nano-hydroxyapatite, Additive Manufacturing, 34 (2020) 101305.

[108] G. Wu, B. Zhou, Y. Bi, Y. Zhao, Selective laser sintering technology for customized fabrication of facial prostheses, The Journal of Prosthetic Dentistry, 100 (2008) 56-60.

[109] G.V. Salmoria, P. Klauss, C.R. Roesler, L.A. Kanis, Structure and Mechanical Properties of PCL/PG Devices Prepared by Selective Laser Sintering for Drug Delivery Applications, ASME 2013 Summer Bioengineering Conference, American Society of Mechanical Engineers Digital Collection, 2013.

[110] G.V. Salmoria, P. Klauss, K. Zepon, L.A. Kanis, C.R.M. Roesler, L.F. Vieira, Development of functionally-graded reservoir of PCL/PG by selective laser sintering for drug delivery devices, Virtual and Physical Prototyping, 7 (2012) 107-115.

[111] I. Ghebre-Sellassie, A. Knoch, Pelletization techniques, in: J. Swarbrick (Ed.) Encyclopedia of Pharmaceutical Technology, Informa Healthcare USA, Inc, New York, 2007, pp. 2651-2663.

[112] G.V. Salmoria, M.R. Cardenuto, C.R.M. Roesler, K.M. Zepon, L.A. Kanis, PCL/Ibuprofen Implants Fabricated by Selective Laser Sintering for Orbital Repair, Procedia CIRP, 49 (2016) 188-192.

[113] G. Salmoria, F. Vieira, G. Ghizoni, I. Gindri, L. Kanis, Additive Manufacturing of PE/Fluorouracil Waffles for Implantable Drug Delivery in Bone Cancer Treatment, International Journal of Engineering Research and Science, 3 (2017) 62-70.

[114] G. Salmoria, F. Vieira, G. Ghizoni, M. Marques, L. Kanis, 3D printing of PCL/Fluorouracil tablets by selective laser sintering: Properties of implantable drug delivery for cartilage cancer treatment, drugs, 2 (2017) 1-7.

[115] A. Goyanes, U. Det-Amornrat, J. Wang, A.W. Basit, S. Gaisford, 3D scanning and 3D printing as innovative technologies for fabricating personalized topical drug delivery systems, J. Control. Release, 234 (2016) 41-48.

[116] Z. Muwaffak, A. Goyanes, V. Clark, A.W. Basit, S.T. Hilton, S. Gaisford, Patient-specific 3D scanned and 3D printed antimicrobial polycaprolactone wound dressings, Int J Pharm, 527 (2017) 161-170.

[117] B. Redwood, How to design parts for metal 3D printing, 2020. https://www.3dhubs.com/knowledge-base/how-design-parts-metal-3d-printing/#process.

[118] A.B. Varotsis, Introduction to metal 3D printing, 2020. https://www.3dhubs.com/knowledge-base/introduction-metal-3d-printing/.

[119] B. Mueller, T. Toeppel, M. Gebauer, R. Neugebauer, Innovative features in implants through beam melting—a new approach for additive manufacturing of endoprostheses, Innovative Developments in Virtual and Physical Prototyping, (2012) 519-523.

[120] Y.-H. Chueh, C. Wei, X. Zhang, L. Li, Integrated laser-based powder bed fusion and fused filament fabrication for three-dimensional printing of hybrid metal/polymer objects, Additive Manufacturing, 31 (2020) 100928.

[121] D.S. Dunn, S. Raghavan, R.G. Volz, Gentamicin sulfate attachment and release from anodized Ti-6Al-4V orthopedic materials, Journal of Biomedical Materials Research, 27 (1993) 895-900.

[122] Y. Zheng, Q. Han, J. Wang, D. Li, Z. Song, J. Yu, Promotion of Osseointegration between Implant and Bone Interface by Titanium Alloy Porous Scaffolds Prepared by 3D Printing, ACS Biomaterials Science & Engineering, 6 (2020) 5181-5190.

[123] H. Hassanin, L. Finet, S.C. Cox, P. Jamshidi, L.M. Grover, D.E.T. Shepherd, O. Addison, M.M. Attallah, Tailoring selective laser melting process for titanium drug-delivering implants with releasing micro-channels, Additive Manufacturing, 20 (2018) 144-155.

[124] M.B. Bezuidenhout, E. Booysen, A.D. van Staden, E.H. Uheida, P.A. Hugo, G.A. Oosthuizen, D.M. Dimitrov, L.M.T. Dicks, Selective Laser Melting of Integrated Ti6Al4V ELI Permeable Walls for Controlled Drug Delivery of Vancomycin, ACS Biomaterials Science & Engineering, 4 (2018) 4412-4424.

[125] I.A.J. van Hengel, M. Riool, L.E. Fratila-Apachitei, J. Witte-Bouma, E. Farrell, A.A. Zadpoor, S.A.J. Zaat, I. Apachitei, Selective laser melting porous metallic implants with immobilized silver nanoparticles kill and prevent biofilm formation by methicillin-resistant Staphylococcus aureus, Biomaterials, 140 (2017) 1-15.

[126] C. Flege, F. Vogt, S. Höges, L. Jauer, M. Borinski, V.A. Schulte, R. Hoffmann, R. Poprawe, W. Meiners, M. Jobmann, K. Wissenbach, R. Blindt, Development and characterization of a coronary polylactic acid stent prototype generated by selective laser melting, Journal of Materials Science: Materials in Medicine, 24 (2013) 241-255.

[127] S. Guo, Y. Lu, S. Wu, L. Liu, M. He, C. Zhao, Y. Gan, J. Lin, J. Luo, X. Xu, Preliminary study on the corrosion resistance, antibacterial activity and cytotoxicity of selective-laser-melted Ti6Al4V-xCu alloys, Materials Science and Engineering: C, 72 (2017) 631-640.

[128] P. Krakhmalev, I. Yadroitsev, I. Yadroitsava, O. De Smidt, Functionalization of biomedical Ti6Al4V via in situ alloying by cu during laser powder bed fusion manufacturing, Materials, 10 (2017) 1154.

[129] J. Vaithilingam, S. Kilsby, R.D. Goodridge, S.D.R. Christie, S. Edmondson, R.J.M. Hague, Functionalisation of Ti6Al4V components fabricated using selective laser melting with a bioactive compound, Materials Science and Engineering: C, 46 (2015) 52-61.

[130] J. Vaithilingam, S. Kilsby, R.D. Goodridge, S.D.R. Christie, S. Edmondson, R.J.M. Hague, Immobilisation of an antibacterial drug to Ti6Al4V components fabricated using selective laser melting, Applied Surface Science, 314 (2014) 642-654.

[131] N.J. Bassous, C.L. Jones, T.J. Webster, 3-D printed Ti-6Al-4V scaffolds for supporting osteoblast and restricting bacterial functions without using drugs: Predictive equations and experiments, Acta Biomaterialia, 96 (2019) 662-673.

[132] L. Ciocca, M. Fantini, F. De Crescenzio, G. Corinaldesi, R. Scotti, Direct metal laser sintering (DMLS) of a customized titanium mesh for prosthetically guided bone regeneration of atrophic maxillary arches, Medical & Biological Engineering & Computing, 49 (2011) 1347-1352.

[133] M. Larosa, A. Jardini, L. Bernardes, M.W. Maciel, R. Maciel Filho, C. Zaváglia, F. Zaváglia, D. Calderoni, P. Kharmandayan, Custom-built implants manufacture in titanium alloy by Direct Metal Laser Sintering (DMLS), High Value Manufacturing: Advanced Research in Virtual and Rapid Prototyping: Proceedings of the 6th International Conference on Advanced Research in Virtual and Rapid Prototyping, Leiria, Portugal, 1-5 October, 2013, CRC Press, 2013, pp. 297.

[134] D.M. Chernogorskyi, M.V. Voller, A.S. Vasilyev, Y.V. Chepurnyi, A.V. Kopchak, Clinical Efficacy of Patient-specific Implants Manufactured by Direct Metal Laser Sintering (DMLS) Technology in Patients with Mandibular Defects, J DIAGN TREAT ORAL MAXILLOFAC PATHOL, 4 162–177.

[135] B. Guan, H. Wang, R. Xu, G. Zheng, J. Yang, Z. Liu, M. Cao, M. Wu, J. Song, N. Li, T. Li, Q. Cai, X. Yang, Y. Li, X. Zhang, Establishing Antibacterial Multilayer Films on the Surface of Direct Metal Laser Sintered Titanium Primed with Phase-Transited Lysozyme, Scientific Reports, 6 (2016) 36408.

[136] G.-N. Ahn, T. Yu, H.-J. Lee, K.-W. Gyak, J.-H. Kang, D. You, D.-P. Kim, A numbering-up metal microreactor for the high-throughput production of a commercial drug by copper catalysis, Lab on a chip, 19 (2019) 3535-3542.

[137] C.A. Terrazas, S.M. Gaytan, E. Rodriguez, D. Espalin, L.E. Murr, F. Medina, R.B. Wicker, Multi-material metallic structure fabrication using electron beam melting, The International Journal of Advanced Manufacturing Technology, 71 (2014) 33-45.

[138] S. Rossi, A. Puglisi, M. Benaglia, Additive Manufacturing Technologies: 3D Printing in Organic Synthesis, ChemCatChem, 10 (2018) 1512-1525.

[139] M. Jamshidinia, M.M. Atabaki, M. Zahiri, S. Kelly, A. Sadek, R. Kovacevic, Microstructural modification of Ti–6Al–4V by using an in-situ printed heat sink in Electron Beam Melting® (EBM), Journal of Materials Processing Technology, 226 (2015) 264-271.

[140] W.J. Sames, F.A. List, S. Pannala, R.R. Dehoff, S.S. Babu, The metallurgy and processing science of metal additive manufacturing, International Materials Reviews, 61 (2016) 315-360.

[141] L.E. Murr, S.M. Gaytan, D.A. Ramirez, E. Martinez, J. Hernandez, K.N. Amato, P.W. Shindo, F.R. Medina, R.B. Wicker, Metal Fabrication by Additive Manufacturing Using Laser and Electron Beam Melting Technologies, Journal of Materials Science & Technology, 28 (2012) 1-14.

[142] H.K. Rafi, N.V. Karthik, H. Gong, T.L. Starr, B.E. Stucker, Microstructures and Mechanical Properties of Ti6Al4V Parts Fabricated by Selective Laser Melting and Electron Beam Melting, Journal of Materials Engineering and Performance, 22 (2013) 3872-3883.

[143] L. Murr, Additive manufacturing of biomedical devices: an overview, Materials technology, 33 (2018) 57-70.

[144] M. Cronskär, M. Bäckström, L.E. Rännar, Production of customized hip stem prostheses–a comparison between conventional machining and electron beam melting (EBM), Rapid Prototyping Journal, 19 (2013) 365–372.

[145] L.E. Murr, Open-cellular metal implant design and fabrication for biomechanical compatibility with bone using electron beam melting, Journal of the Mechanical Behavior of Biomedical Materials, 76 (2017) 164-177.

[146] M.B. Bezuidenhout, D.M. Dimitrov, A.D. van Staden, G.A. Oosthuizen, L.M.T. Dicks, Titanium-Based Hip Stems with Drug Delivery Functionality through Additive Manufacturing, BioMed Research International, 2015 (2015) 134093.

[147] R. Yan, D. Luo, H. Huang, R. Li, N. Yu, C. Liu, M. Hu, Q. Rong, Electron beam melting in the fabrication of three-dimensional mesh titanium mandibular prosthesis scaffold, Scientific Reports, 8 (2018) 750.

[148] A. Kumar, K.C. Nune, R.D.K. Misra, Biological functionality and mechanistic contribution of extracellular matrix-ornamented three dimensional Ti-6Al-4V mesh scaffolds, Journal of Biomedical Materials Research Part A, 104 (2016) 2751-2763.

[149] K.C. Nune, A. Kumar, L.E. Murr, R.D.K. Misra, Interplay between self-assembled structure of bone morphogenetic protein-2 (BMP-2) and osteoblast functions in three-dimensional titanium alloy scaffolds: Stimulation of osteogenic activity, Journal of Biomedical Materials Research Part A, 104 (2016) 517-532.

[150] H. Liu, W. Li, C. Liu, J. Tan, H. Wang, B. Hai, H. Cai, H.-J. Leng, Z.-J. Liu, C.-L. Song, Incorporating simvastatin/poloxamer 407 hydrogel into 3D-printed porous Ti 6 Al 4 V scaffolds for the promotion of angiogenesis, osseointegration and bone ingrowth, Biofabrication, 8 (2016) 045012.

[151] Z. Liu, P. Zhang, M. Yan, Y. Xie, G. Huang, Additive manufacturing of specific ankle-foot orthoses for persons after stroke: A preliminary study based on gait analysis data, Math. Biosci. Eng, 16 (2019) 8134-8143.

[152] T. Binedell, E. Meng, K. Subburaj, Design and development of a novel 3D-printed non-metallic self-locking prosthetic arm for a forequarter amputation, Prosthetics and Orthotics International, (2020) 0309364620948290.

[153] S.A. Oh, C.M. Lee, M.W. Lee, Y.S. Lee, G.H. Lee, S.H. Kim, S.K. Kim, J.W. Park, J.W. Yea, Fabrication of a Patient-Customized Helmet with a Three-Dimensional Printer for Radiation Therapy of Scalp, Progress in Medical Physics, 28 (2017) 100-105.

[154] A. Pilipović, T. Brajlih, I. Drstvenšek, Influence of Processing Parameters on Tensile Properties of SLS Polymer Product, Polymers, 10 (2018) 1208.

[155] C. Kundera, T. Kozior, Mechanical properties of models prepared by SLS technology, AIP Conference Proceedings, 2017 (2018) 020012.

[156] C. Kundera, T. Kozior, Influence of printing parameters on the mechanical properties of polyamide in SLS technology, Czasopismo Techniczne, 2016 (2016) 31-37.

[157] M. Shehata, T.M. Hatem, W.A. Samad, Experimental Study of Build Orientation in Direct Metal Laser Sintering of 17-4PH Stainless Steel, 3D Printing and Additive Manufacturing, 6 (2018) 227-233.

[158] M.J. Matthews, G. Guss, S.A. Khairallah, A.M. Rubenchik, P.J. Depond, W.E. King, Denudation of metal powder layers in laser powder bed fusion processes, Acta Materialia, 114 (2016) 33-42.

[159] L. Arregui, I. Garmendia, J. Pujana, C. Soriano, Study of the geometrical limitations associated to the metallic part manufacturing by the LMD process, Procedia CIRP, 68 (2018) 363-368.

[160] I. Gibson, D. Shi, Material properties and fabrication parameters in selective laser sintering process, Rapid Prototyping Journal, 3 (1997) 129-136.

[161] J.R.C. Dizon, A.H. Espera, Q. Chen, R.C. Advincula, Mechanical characterization of 3D-printed polymers, Additive Manufacturing, 20 (2018) 44-67.

[162] J. Nelson, N. Vail, Post-processing of selective laser sintered polycarbonate parts, 1991 International Solid Freeform Fabrication Symposium, 1991.

[163] N.K. Tolochko, T. Laoui, Y.V. Khlopkov, S.E. Mozzaharov, V.I. Titov, M.B. Ignatiev, Absorptance of powder materials suitable for laser sintering, Rapid Prototyping Journal, 6 (2000) 155-161.

[164] J.P. Kruth, X. Wang, T.L. and, L. Froyen, Lasers and materials in selective laser sintering, Assembly Automation, 23 (2003) 357-371.

[165] J.P. Bergmann, M. Bielenin, M. Stambke, T. Feustel, P.v. Witzendorff, J. Hermsdorf, Effects of diode laser superposition on pulsed laser welding of aluminum, Physics Procedia, 41 (2013) 180-189.

[166] M. Zavala-Arredondo, N. Boone, J. Willmott, D.T. Childs, P. Ivanov, K.M. Groom, K. Mumtaz, Laser diode area melting for high speed additive manufacturing of metallic components, Materials & Design, 117 (2017) 305-315.

[167] M. Shellabear, O. Nyrhilä, DMLS-Development history and state of the art, Laser Assisted Netshape engineering 4, proceedings of the 4th LANE, (2004) 21-24.

[168] E. Yasa, T. Craeghs, J.-P. Kruth, Selective Laser Sintering/Melting and Selective Laser Erosion with Nd: YAG Lasers, Journal of Optics Research, 14 (2012) 211.

[169] S. Kumar, Laser Powder Bed Fusion, in: S. Kumar (Ed.) Additive Manufacturing Processes, Springer International Publishing, Cham, 2020, pp. 41-63.

[170] L.A. Fred, A. Lohrengel, V. Neubert, F.H. Camila, T. Czelusniak, Selective laser sintering of Mo-CuNi composite to be used as EDM electrode, Rapid Prototyping Journal, 20 (2014) 59-68.

[171] G.V. Salmoria, P. Klauss, R.A. Paggi, L.A. Kanis, A. Lago, Structure and mechanical properties of cellulose based scaffolds fabricated by selective laser sintering, Polymer Testing, 28 (2009) 648-652.

[172] A. Keshavarzkermani, E. Marzbanrad, R. Esmaeilizadeh, Y. Mahmoodkhani, U. Ali, P.D. Enrique, N.Y. Zhou, A. Bonakdar, E. Toyserkani, An investigation into the effect of process parameters on melt pool geometry, cell spacing, and grain refinement during laser powder bed fusion, Optics & Laser Technology, 116 (2019) 83-91.

[173] J. Ciurana, L. Hernandez, J. Delgado, Energy density analysis on single tracks formed by selective laser melting with CoCrMo powder material, The International Journal of Advanced Manufacturing Technology, 68 (2013) 1103-1110.

[174] I. Yadroitsev, I. Smurov, Surface morphology in selective laser melting of metal powders, Physics Procedia, 12 (2011) 264-270.

[175] G.R. Nazami, S. Sahoo, Influence of hatch spacing and laser spot overlapping on heat transfer during laser powder bed fusion of aluminum alloy, Journal of Laser Applications, 32 (2020) 042007.

[176] D. Schulze, Powders and Bulk Solids: Behavior, Characterization, Storage and Flow, Springer, Berlin Heidelberg New York, 2008.

[177] J.M. Williams, A. Adewunmi, R.M. Schek, C.L. Flanagan, P.H. Krebsbach, S.E. Feinberg, S.J. Hollister, S. Das, Bone tissue engineering using polycaprolactone scaffolds fabricated via selective laser sintering, Biomaterials, 26 (2005) 4817-4827.

[178] M. Elbadawi, B. Muñiz Castro, F.K.H. Gavins, J. Jie Ong, S. Gaisford, G. Pérez, A.W. Basit, P. Cabalar, Á. Goyanes, M3DISEEN: A Novel Machine Learning

Approach for Predicting the 3D Printability of Medicines, Int J Pharm, 590 (2020) 119837.

[179] I. Baturynska, O. Semeniuta, K. Martinsen, Optimization of Process Parameters for Powder Bed Fusion Additive Manufacturing by Combination of Machine Learning and Finite Element Method: A Conceptual Framework, Procedia CIRP, 67 (2018) 227-232.

[180] M. Elbadawi, T. Gustaffson, S. Gaisford, A.W. Basit, 3D printing tablets: Predicting printability and drug dissolution from rheological data, Int J Pharm, 590 (2020) 119868.

[181] R. Vehring, Pharmaceutical Particle Engineering via Spray Drying, Pharmaceutical Research, 25 (2008) 999-1022.

[182] Y.-F. Maa, H.R. Costantino, P.-A. Nguyen, C.C. Hsu, The Effect of Operating and Formulation Variables on the Morphology of Spray-Dried Protein Particles, Pharm. Dev. Technol., 2 (1997) 213-223.

[183] R. Hamed, E.M. Mohamed, Z. Rahman, M.A. Khan, 3D-printing of lopinavir printlets by selective laser sintering and quantification of crystalline fraction by XRPD-chemometric models, Int J Pharm, 592 (2021) 120059.

[184] P. Kulinowski, P. Malczewski, E. Pesta, M. Łaszcz, A. Mendyk, S. Polak, P. Dorożyński, Selective laser sintering (SLS) technique for pharmaceutical applications—Development of high dose controlled release printlets, Additive Manufacturing, 38 (2021) 101761.

[185] Y. Yang, Y. Xu, S. Wei, W. Shan, Oral preparations with tunable dissolution behavior based on selective laser sintering technique, Int J Pharm, 593 (2021) 120127.

[186] Y.A. Gueche, N.M. Sanchez-Ballester, B. Bataille, A. Aubert, L. Leclercq, J.-C. Rossi, I. Soulairol, Selective Laser Sintering of Solid Oral Dosage Forms with Copovidone and Paracetamol Using a CO2 Laser, Pharmaceutics, 13 (2021).

[187] G.V. Salmoria, P. Klauss, K.M. Zepon, L.A. Kanis, The effects of laser energy density and particle size in the selective laser sintering of polycaprolactone/progesterone specimens: morphology and drug release, The International Journal of Advanced Manufacturing Technology, 66 (2013) 1113-1118.

[188] G. Salmoria, P. Klauss, L. Kanis, Laser Printing of PCL/Progesterone Tablets for Drug Delivery Applications in Hormone Cancer Therapy, Lasers in Manufacturing and Materials Processing, 4 (2017) 108-120.

[189] G. Salmoria, P. Klauss, K. Zepon, L. Kanis, C. Roesler, L. Vieira, Development of functionally-graded reservoir of PCL/PG by selective laser sintering for drug delivery devices: This paper presents a selective laser sintering-fabricated drug delivery system that contains graded progesterone content, Virtual and Physical Prototyping, 7 (2012) 107-115.

[190] C. Telenko, C.C. Seepersad, Assessing energy requirements and material flows of selective laser sintering of Nylon parts, Proceedings of the Solid Freeform Fabrication Symposium, 2010, pp. 8-10.08.

[191] K. Dotchev, W. Yusoff, Recycling of polyamide 12 based powders in the laser sintering process, Rapid Prototyping Journal, 15 (2009) 192-203.

[192] H.P. Tang, M. Qian, N. Liu, X.Z. Zhang, G.Y. Yang, J. Wang, Effect of Powder Reuse Times on Additive Manufacturing of Ti-6Al-4V by Selective Electron Beam Melting, JOM, 67 (2015) 555-563.

[193] A.N.D. Gasper, B. Szost, X. Wang, D. Johns, S. Sharma, A.T. Clare, I.A. Ashcroft, Spatter and oxide formation in laser powder bed fusion of Inconel 718, Additive Manufacturing, 24 (2018) 446-456.

[194] D.S. Thomas, S.W. Gilbert, Costs and cost effectiveness of additive manufacturing, NIST special publication, 1176 (2014) 12.

[195] A. Khorasani, I. Gibson, J.K. Veetil, A.H. Ghasemi, A review of technological improvements in laser-based powder bed fusion of metal printers, The International Journal of Advanced Manufacturing Technology, 108 (2020) 191-209.

[196] E. MacDonald, R. Wicker, Multiprocess 3D printing for increasing component functionality, Science, 353 (2016) aaf2093.

[197] P. Edwards, M. Ramulu, Fatigue performance evaluation of selective laser melted Ti–6Al–4V, Materials Science and Engineering: A, 598 (2014) 327-337.

[198] J. Norman, R.D. Madurawe, C.M.V. Moore, M.A. Khan, A. Khairuzzaman, A new chapter in pharmaceutical manufacturing: 3D-printed drug products, Advanced Drug Delivery Reviews, 108 (2017) 39-50.

[199] U.S. Food and Drug Administration, Technical considerations for additive manufactured medical devices, 2017. https://www.fda.gov/regulatory-information/search-fda-guidance-documents/technical-considerations-additive-manufactured-medical-devices.

[200] X. Xu, A. Awad, P.R. Martinez, S. Gaisford, A. Goyanes, A.W. Basit, Vat photopolymerization 3D printing for advanced drug delivery and medical device applications, Journal of Controlled Release, 329 (2020) 743-757.

[201] U.S. Food And Drug Administration, Guidance for Industry: PAT—a framework for innovative pharmaceutical development, manufacturing, and quality assurance, Rockville, MD, (2004).

[202] C.J. Strachan, T. Rades, K.C. Gordon, J. Rantanen, Raman spectroscopy for quantitative analysis of pharmaceutical solids, Journal of Pharmacy and Pharmacology, 59 (2007) 179-192.

[203] A. Paudel, D. Raijada, J. Rantanen, Raman spectroscopy in pharmaceutical product design, Adv. Drug Deliv. Rev., 89 (2015) 3-20.

[204] M. Edinger, L.-D. Iftimi, D. Markl, M. Al-Sharabi, D. Bar-Shalom, J. Rantanen, N. Genina, Quantification of Inkjet-Printed Pharmaceuticals on Porous Substrates Using Raman Spectroscopy and Near-Infrared Spectroscopy, AAPS PharmSciTech, 20 (2019) 207.

[205] S.J. Trenfield, A. Goyanes, R. Telford, D. Wilsdon, M. Rowland, S. Gaisford, A.W. Basit, 3D printed drug products: Non-destructive dose verification using a rapid point-and-shoot approach, Int J Pharm, 549 (2018) 283-292.

[206] Z. Rahman, S.F. Barakh Ali, T. Ozkan, N.A. Charoo, I.K. Reddy, M.A. Khan, Additive Manufacturing with 3D Printing: Progress from Bench to Bedside, The AAPS Journal, 20 (2018) 101.

[207] Z. Rahman, A. Mohammad, S. Akhtar, A. Siddiqui, M. Korang-Yeboah, M.A. Khan, Chemometric Model Development and Comparison of Raman and 13C Solid-State Nuclear Magnetic Resonance–Chemometric Methods for Quantification of Crystalline/Amorphous Warfarin Sodium Fraction in the Formulations, J. Pharm. Sci., 104 (2015) 2550-2558.

[208] A. Siddiqui, Z. Rahman, V.A. Sayeed, M.A. Khan, Chemometric Evaluation of Near Infrared, Fourier Transform Infrared, and Raman Spectroscopic Models for the Prediction of Nimodipine Polymorphs, J. Pharm. Sci., 102 (2013) 4024-4035.

[209] A. Melocchi, F. Briatico-Vangosa, M. Uboldi, F. Parietti, M. Turchi, D. von Zeppelin, A. Maroni, L. Zema, A. Gazzaniga, A. Zidan, Quality considerations on the pharmaceutical applications of fused deposition modeling 3D printing, Int J Pharm, 592 (2021) 119901.

[210] S.J. Trenfield, H. Xian Tan, A. Goyanes, D. Wilsdon, M. Rowland, S. Gaisford, A.W. Basit, Non-destructive dose verification of two drugs within 3D printed polyprintlets, Int J Pharm, 577 (2020) 119066.

[211] H. Vakili, R. Kolakovic, N. Genina, M. Marmion, H. Salo, P. Ihalainen, J. Peltonen, N. Sandler, Hyperspectral imaging in quality control of inkjet printed personalised dosage forms, Int J Pharm, 483 (2015) 244-249.

[212] J. Aho, J.P. Bøtker, N. Genina, M. Edinger, L. Arnfast, J. Rantanen, Roadmap to 3D-Printed Oral Pharmaceutical Dosage Forms: Feedstock Filament Properties and Characterization for Fused Deposition Modeling, J. Pharm. Sci., 108 (2019) 26-35.

[213] N. Sandler, I. Kassamakov, H. Ehlers, N. Genina, T. Ylitalo, E. Haeggstrom, Rapid interferometric imaging of printed drug laden multilayer structures, Scientific Reports, 4 (2014) 4020.

[214] Merck, TRANSFORM YOUR CLINICAL TRIALS SUPPLY FROM COMPLEX TO EASY, 2021. https://www.merckgroup.com/en/research/innovation-center/highlights/onezeromed.html.

[215] A. Goyanes, C.M. Madla, A. Umerji, G. Duran Piñeiro, J.M. Giraldez Montero, M.J. Lamas Diaz, M. Gonzalez Barcia, F. Taherali, P. Sánchez-Pintos, M.-L. Couce, S. Gaisford, A.W. Basit, Automated therapy preparation of isoleucine formulations

using 3D printing for the treatment of MSUD: First single-centre, prospective, crossover study in patients, Int J Pharm, 567 (2019) 118497.

[216] M. Hay, D.W. Thomas, J.L. Craighead, C. Economides, J. Rosenthal, Clinical development success rates for investigational drugs, Nat Biotechnol, 32 (2014) 40-51.